Journal of Controlled Release 172 (2013) 782–794

Contents lists available at ScienceDirect

Journal of Controlled Release

journal homepage: www.elsevier.com/locate/jconrel

Review

Factors controlling the pharmacokinetics, biodistribution and intratumoral penetration of nanoparticles

Mark J. Ernsting [a,b], Mami Murakami [a], Aniruddha Roy [a], Shyh-Dar Li [a,c,d,*]

[a] Drug Delivery and Formulation, Drug Discovery Program, Ontario Institute for Cancer Research, 101 College Street, Suite 800, Toronto, Ontario M5G 0A3, Canada
[b] Ryerson University, Faculty of Architectural Science and Engineering, Toronto, Ontario M5B 1Z2, Canada
[c] Leslie Dan Faculty of Pharmacy, University of Toronto, Toronto, Ontario M5S 3M2, Canada
[d] The Techna Institute, University Health Network, Toronto, Ontario M5G 1P5, Canada

ARTICLE INFO

Article history:
Received 7 August 2013
Accepted 15 September 2013
Available online 25 September 2013

Keywords:
Nanoparticle
Pharmacokinetics
Biodistribution
Tumor microenvironment
Intratumoral penetration

ABSTRACT

Nanoparticle drug delivery to the tumor is impacted by multiple factors: nanoparticles must evade clearance by renal filtration and the reticuloendothelial system, extravasate through the enlarged endothelial gaps in tumors, penetrate through dense stroma in the tumor microenvironment to reach the tumor cells, remain in the tumor tissue for a prolonged period of time, and finally release the active agent to induce pharmacological effect. The physicochemical properties of nanoparticles such as size, shape, surface charge, surface chemistry (PEGylation, ligand conjugation) and composition affect the pharmacokinetics, biodistribution, intratumoral penetration and tumor bioavailability. On the other hand, tumor biology (blood flow, perfusion, permeability, interstitial fluid pressure and stroma content) and patient characteristics (age, gender, tumor type, tumor location, body composition and prior treatments) also have impact on drug delivery by nanoparticles. It is now believed that both nanoparticles and the tumor microenvironment have to be optimized or adjusted for optimal delivery. This review provides a comprehensive summary of how these nanoparticle and biological factors impact nanoparticle delivery to tumors, with discussion on how the tumor microenvironment can be adjusted and how patients can be stratified by imaging methods to receive the maximal benefit of nanomedicine. Perspectives and future directions are also provided.

Contents

* Corresponding author at: 101 College St, MaRS Centre South Tower, Suite 800, Toronto, Ontario M5G 0A3, Canada. Tel.: +1 647 260 7994.
E-mail address: sli@oicr.on.ca (S.-D. Li).

0168-3659/$ – see front matter © 2013 Elsevier B.V. All rights reserved.
http://dx.doi.org/10.1016/j.jconrel.2013.09.013

1. Introduction

Nanomedicine therapies are broadly defined as active pharmaceutical ingredients formulated in delivery vehicles exhibiting an average size between 10 and 200 nm, and these encompass liposomes, micelles, polymeric nanoparticles, dendrimers, and macromolecules. Properly formulated nanoparticles evade the 5 nm renal filtration cutoff [1–3] and exhibit prolonged blood circulation, giving these particles an increased opportunity to interact with tumor tissues. Unlike normal blood vessels which feature a tightly sealed endothelium, tumor vasculature tends to be abnormally permeable to macromolecules and nanoparticles, and furthermore, lymphatic drainage is generally impaired in tumors: as a result of these pathological features, nanoparticles selectively accumulate in this biological cul-de-sac. On the other hand, low molecular weight drugs can non-selectively diffuse through the endothelial layer of normal tissues, inducing significant off-target toxicity at therapeutic doses. The enhanced permeability and retention (EPR) effect is the central hypothesis and science of nanomedicine, and tumors that present with high permeability are good candidates for this class of therapy.

Nanoparticles display distinctive pharmacokinetics (PK) and biodistribution (BD) compared to small molecules, and the altered *in vivo* biofate in turn alters the toxicity and efficacy profile of each drug. There are three major phases in nanoparticle drug delivery (Fig. 1): (1) systemic circulation and reticuloendothelial system (RES) interaction, (2) extravasation and tumor penetration, and lastly, (3) interaction with the target cells. This review focuses on the effect of nanoparticle composition and physicochemical properties on the interactions with the biological systems in these three phases, and how those interactions affect nanoparticle biofate.

2. Blood circulation and RES interaction

The first phase of delivery involves the systemic circulation and interaction with the RES, a global system of macrophages in the liver, spleen, and bone marrow, but with respect to nanoparticle clearance, the liver and spleen are the most active. Macrophages are phagocytic cells, and will engulf particles bearing recognized opsonins (serum proteins) that have adsorbed to nanoparticles [4–6]. For example, Nagayama et al. [7] demonstrated that the increased amount of complement protein C3 and immunoglobulin G (IgG) adsorbed onto the 50-nm polystyrene nanoparticles in the serum was directly reflected in the increased rate of uptake of the nanoparticles by Kupffer cells. Factors affecting opsonization and the RES interaction include PEGylation, size, composition, zeta potential, and shape of nanoparticles. Interaction of nanoparticles with the RES is a significant determinant of blood circulation time and rates of clearance. Nanoparticles with a decreased blood circulation time usually display reduced tumor uptake and efficacy.

2.1. Strategies to reduce RES interactions

2.1.1. Surface decoration

The most widely used surface decoration technique is introduction of polyethylene glycol (PEG), which is a hydrophilic polymer, to the surface of nanoparticles to reduce serum protein binding through a process of steric hindrance. PEG has been deployed in various types of nanoparticles, including liposomes, polymeric nanoparticles, and hybrid nanoparticles [8]. Sadzuko et al. [9] reported that PEGylation led to a 3-fold reduction in RES uptake, a 6-fold higher plasma area under the curve (AUC), and a 3-fold increased tumor uptake of a liposomal drug, leading to enhanced antitumor efficacy. Similar results have been reported by others with different types of nanoparticles [10–12]. PEG creates a border around nanoparticles and provides a nonspecific steric hindrance barrier preventing access of proteins [13,14]. The molecular weight (MW) of PEG and the amount used has an influence on performance. Fang et al. [15] studied protein adsorption on 100–200 nm PEGylated nanoparticles containing a range of PEG MW (2, 5, and 10 kDa), and determined that 10 kDa PEG was the most effective. Ernsting et al. [16] prepared PEGylated cellulose drug conjugates which exhibited self-assembly properties dependent on hydrophobic/hydrophilic balance, and for this system a 2 kDa PEG was optimal. Walkey et al. [17] utilized label-free liquid chromatography tandem mass spectrometry to determine serum protein binding to gold nanoparticles possessing different surface PEG densities. They reported that gold nanoparticles with different PEG densities attract different clusters of serum proteins, and the cluster of proteins binding to low PEG density particles (<0.16 PEG/nm^2) facilitated macrophage uptake. On the other hand, the cluster of proteins that bound to high PEG density particles (>0.64 PEG/nm^2) did not trigger serum-dependent phagocytosis, and the uptake by macrophage was less efficient (Fig. 2). While PEG reduces RES interactions, PEG also has an impact on particle properties including stability and drug release, and for each composition the MW and wt.% of PEG have to be experimentally optimized. This is a well-known consideration in liposomal formulation: DSPE-PEG$_{2000}$ is a common component of PEGylated liposomes, but it has detergent properties, and will destabilize liposomes when exceeding 8 mol% [18].

Despite the benefits that PEG confers, PEGylation is suspected to induce immune responses and hypersensitivity, especially when an immunostimulatory agent is included such as siRNA and pDNA [19–21]. Ishida et al. [22] and Judge et al. [23] demonstrated that the

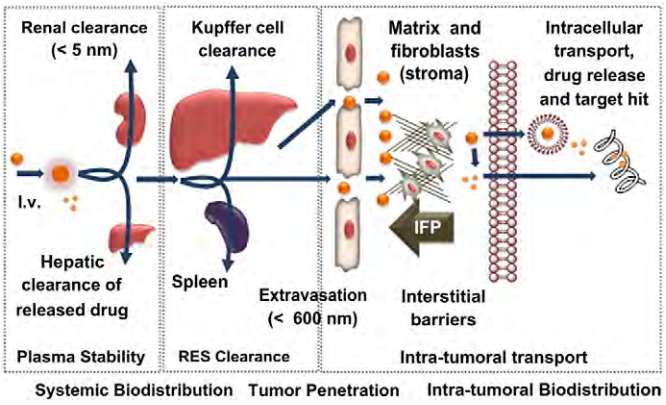

Fig. 1. The three phases of drug delivery by nanoparticles. Nanoparticles injected intravenously must evade RES and renal clearance, and remain stable in plasma during systemic circulation, such that a sufficient dose of nanoparticle and drug can interact with tumor physiology. Once particles successfully extravasate into the tumor compartment, the particles must travel through the stroma against high interstitial fluid pressure (IFP) gradients, and ultimately interact with the target cells or release the drug payload for pharmacological effect.

blood clearance of the second dose of PEGylated liposomes was accelerated by spleen-dependent generation of specific anti-PEG IgM. Exploration of alternative compositions to PEG is a relatively small field. Polyamino acids (such as polyglutamic acid), glycopolymers, and polyoxazolines (POx) have been shown to assist molecules and nanoparticles to evade RES clearance [24,25].

Regardless of the mechanism by which PEG works and how well it improves PK and BD, significant RES clearance is still an issue, with typically >50% of the injected dose (ID) ending up in the liver and spleen after 48 h even for highly optimized PEGylated particles [13,14,26,27].

Rodriguez and colleagues [28] conjugated a "Self" peptide on to the surface of a nanoparticle, and demonstrated that the macrophage-mediated clearance of the nanoparticles was reduced, leading to >10-fold prolonged blood circulation and ~4-fold increased tumor uptake compared to the standard PEGylated nanoparticles. The "Self" peptide was computationally designed to mimic the function of human CD47, which is a marker of self, impeding phagocytosis of self by signaling through the phagocyte receptor CD172a.

2.1.2. Size and morphology

For a nanoparticle to exhibit prolonged circulation and leverage the EPR effect, the lower limit of particle size is 5.5 nm, the renal filtration cutoff size [29]. A second lower limit is imposed by liver filtration, as vascular fenestrations in the liver are 50–100 nm, and particles smaller than 50 nm will interact with hepatocytes. The upper limit of particle size is influenced by two factors: tumor permeability and splenic filtration. Vascular fenestrations vary from 400 to 600 nm to microns [30] among tumors. Liu et al. [4] investigated the BD of liposomes ranging from 30 to 400 nm: 4 h after injection, liposomes ranging from 100 to 200 nm were 4-fold more concentrated in tumors compared to liposomes below 50 and above 300 nm. The liver uptake of particles below 50 and above 300 nm was 25% ID, compared to 10% ID for 100 nm liposomes. Further, particles greater than 400 nm in size were cleared in the spleen (40–50% ID). Blood components passing through the splenic sinus must pass through intercellular slits that rarely exceed 500 nm in width [31] and although the size cutoff for each nanoparticle will depend on deformability and shape, particles exceeding 300–400 nm tend to be trapped [32]. Hrkach et al. [33] generated a comprehensive series of PEG-polyester nanoparticles, examining 63 compositions ranging from 28 to 224 nm, ultimately selecting their lead formulation which was 100 nm in size. Generally, particles near 100 nm in diameter tend to represent an optimal range for leveraging the EPR effect and minimizing clearance [3]. Within a specific class of composition, size will impact protein adsorption and the resulting RES clearance. Fang et al. [15] reported that the protein adsorption on the 80-nm particles (6%) was lower than that on larger sizes (171 and 243 nm, 23 and 34%, respectively), because smaller particles exhibit a higher surface density of PEG. As a result, blood clearance of the 80 nm particles was twice as slow as with the larger nanoparticles (171 and 243 nm). Moreover, the accumulation of the 80 nm particles in the tumor within 24 h was 2-fold that of the larger nanoparticle formulations.

Particle shape is also a crucial parameter that can impact circulation time and tumor accumulation. Champion and Mitragotri [34] measured the interaction of diversely shaped micro-sized polystyrene particles with macrophages. They defined a dimensionless shape-dependent parameter related to the length normalized curvature, Ω (Fig. 3). Particles were found to be internalized successfully when $\Omega \leq 45°$ (ellipsoid or sphere) *via* actin-cup and ring formation, with phagocytosis velocity being inversely correlated to Ω (up to 45°); on the other hand, when $\Omega > 45°$ (ellipsoid), cell spreading but not internalization occurs (Fig. 3). In contrast, the contribution of particle size or volume to the phagocytotic process was evidently lower compared to particle shape, affecting the completion of particle internalization only when the particle volume is greater than that of the macrophage at Ω of ≤45°. They also demonstrated that a form of worm-like polysytrene particles was phagocytosed to a lesser extent by alveolar rat macrophages compared to spherical particles of equal volume. The success of the high aspect ratio particles in avoiding phagocytosis was attributed to the predominance of low curvature regions on the flat sides ($\Omega = 87.5°$) over the high curvature regions ($\Omega = 2.5°$), which were only present at the two discrete ends of the worm-like particles [35].

Altering particle shape away from the spherical has been shown to enhance circulation time and influence particle disposition, as these particles exhibit altered hydrodynamic behavior that influences circulation, transport in the blood flow, and finally BD. Discher and coworkers [36] prepared filamentous micelles (filomicelles) under simulated splenic flow conditions, in which long filomicelles were formed by a solvent evaporation self-assembly process using diblock copolymers of PEG and the inert poly(ethylethylene) or biodegradable poly(ε-caprolactone): the filomicelles exhibited reduced uptake by macrophages, and exhibited persistent circulation for up to a week, which was in strong contrast with the spherical PEGylated stealth vesicles that were cleared within 2 days.

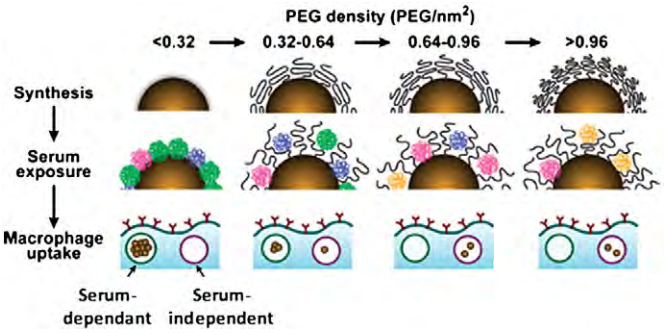

Fig. 2. Schematic illustrating the influence of PEG density on serum protein absorption to gold nanoparticles and their subsequent uptake by macrophages. The top panel shows as-synthesized gold nanoparticles grafted with PEG at increasing density. As PEG density increases, PEG volume decreases as a result of PEG–PEG steric interactions. The middle panel illustrates how PEG density determines the amount and relative abundance of serum proteins absorbed to the gold nanoparticle surface after serum exposure. At low PEG densities (<0.32 PEG/nm^2), proteins from cluster (green) adsorb preferentially. At low-intermediate densities (0.32–0.64 PEG/nm^2), proteins from cluster B (blue) adsorb preferentially. At intermediate-high PEG densities (0.64–0.96 PEG/nm^2), proteins from cluster C (fuchsia) adsorb preferentially. At high PEG densities (>0.96 PEG/nm^2), proteins from cluster D (orange) adsorb preferentially. The lower panel shows that at low PEG densities, macrophage uptake is efficient and serum-dependent. At high PEG densities, macrophage uptake is driven predominantly by a less efficient serum-independent mechanism. Structures in the diagram are conceptualized for illustrative purposes. Adapted from ref [17].

The unique hydrodynamic properties of filamentous, flexible micelles allowed them to align with the blood flow, resulting in a substantial extension of the circulation time [36]. In another example, the circulation time of liposomes in the size range of 100–150 nm was enhanced by 3.6-fold *via* the transformation of the spherical vesicles into a disk-like vesicle [37].

2.1.3. Composition

Material hydrophobicity is commonly associated with the binding of plasma proteins [38,39]. Semple et al. [40,41] demonstrated that liposomes composed of neutral saturated lipids with carbon chains greater than C16 bound to larger quantities of blood proteins compared with their C14 counterparts. Moghimi et al. [42] demonstrated that the liposomes rich in cholesterol bound less protein than cholesterol-free liposomes due to increased rigidity in the lipid bilayer. Lipids present in the liposomes also affect the pharmacokinetic parameters. It has been shown that circulation half-life of liposomes typically increases as a function of increasing lipid dose [43,44]. This effect is likely due to a decreased phagocytic capacity of RES macrophages after the ingestion of high lipid doses or to saturation of opsonization of the circulating liposomes [45].

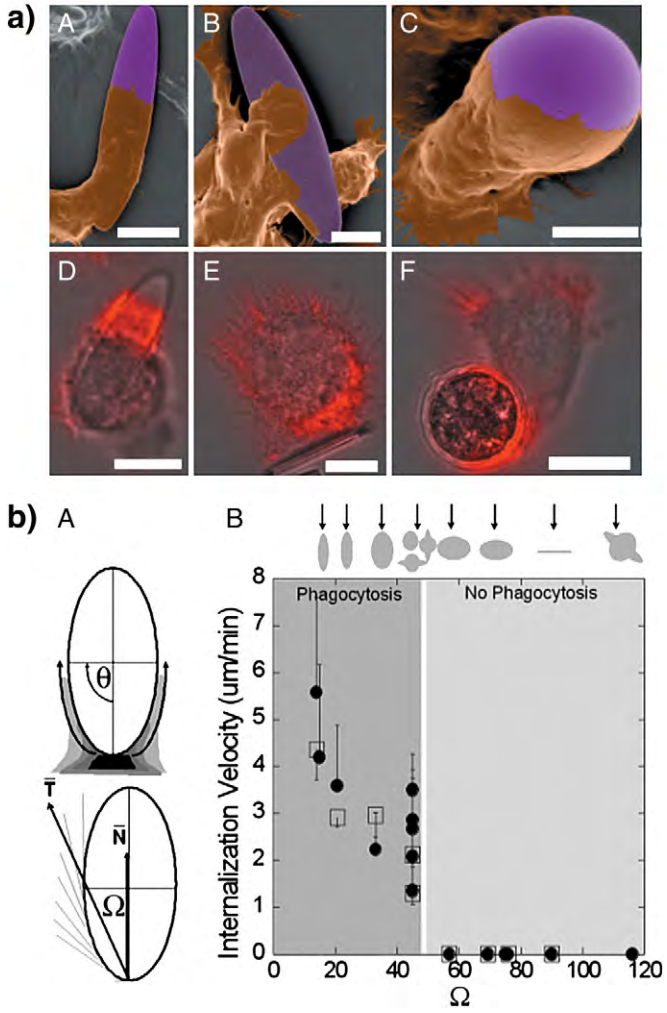

Fig. 3. Effect of target geometry in phagocytosis. (a) Scanning electron micrographs (A–C) of cells and particles were colored brown and purple, respectively. D–F are overlays of bright field and fluorescent images after fixing the cells and staining for polymerized actin with rhodamine phalloidin. A and C: The membrane has progressed down the length of the particle. B: The macrophage has spread over the flat side of an elliptical disk. D and F: Actin ring and cup, respectively, were formed as internalization begins after attachment. E: Actin polymerization occurred in the cell at site of attachment to flat side of an opsonized elliptical disk, but no actin ring or cup was visible. (b) Definition of Ω and its relation with membrane velocity. Ŧ represents the average of tangential angles near the point of cell contact. Ω is the angle between Ŧ and the membrane normal at the site of attachment. Adapted from ref [34]. Copyright (2006) National Academy of Science, USA.

2.1.4. Zeta potential

The net charge on a surface of a particle is measured as zeta potential (ξ), and is an influential physical factor impacting PK and BD. Generally speaking, negative particles ($\xi \leq 10$ mV) exhibit strong RES uptake, and positive particles ($\xi > 10$ mV) will induce serum protein aggregation: neutral nanoparticles (within ± 10 mV) exhibit the least RES interaction and the longest circulation [3]. Semple et al. [40,41] showed that cationic liposomes bind 500–900 serum protein/mol lipid compared to 100 serum protein/mol lipid bound by their neutral counterparts. Xiao et al. [46] demonstrated that nanoparticles with high positive (>10 mV) or negative surface charge (≤10 mV) were efficiently opsonized and cleared by the Kupffer cells from the blood circulation. Levchenko et al. [47] reported similar results: particles exhibiting $\xi \leq 40$ mV exhibited >90% clearance in 10 min compared to <10% clearance for the neutral particles ($\xi \pm 10$ mV), and increased liver uptake (60% ID *versus* <20%ID in 1 h) was implicated in the accelerated clearance. Gessner et al. [48,49] observed an increase in plasma protein adsorption with increasing surface charge density for negatively charged polymeric nanoparticles. They also demonstrated that positively charged polystyrene nanoparticles predominantly adsorb proteins with an isoelectric point (pI) <5.5, such as albumin, while negatively charged particles adsorb proteins with a pI > 5.5, such as IgG [48,49]. Zhang et al. [50] reported that lipoplex (a positively charged complex) formed aggregates in serum, leading to transient embolism in the lungs, with ultimate clearance to the liver. In the Levchenko and Zhang studies, PEGylation served to shield the charge effect [47,50], suggesting that PEG may minimize opsonization not only through steric hindrance but also charge shielding.

2.2. RES activity and personalized dose adjustment

Nanoparticles are cleared largely by the RES [3,51,52]. Therefore, reduced RES activity will result in prolonged blood circulation of nanoparticles, which will have an increased chance to interact with other normal tissues, inducing side effects. La-Beck et al. [53] demonstrated that patients with increased RES activity (increased pre-cycle monocyte count) exhibited enhanced clearance for Doxil, which is a PEGylated liposomal doxorubicin. Therefore, an individual with reduced RES activity will display decreased clearance and increased toxicity, whereas a patient exhibiting high RES activity will experience increased clearance and reduced efficacy at the same dose. These results suggest that: first, individual dose adjustment according to the RES activity (possibly *via* pre-cycle monocyte count) is needed to optimize the treatment and minimize the side effects of nanomedicines. Second, multiple dosing should be planned carefully as the interaction between nanoparticles and the RES is bi-directional [54]: the first dose of nanoparticles may suppress the RES activity, reducing the clearance and increasing the toxicity of the subsequent doses. For example, the blood clearance of Doxil in human patients was shown to be reduced by 43% at the third dose compared to the first dose, and the skin toxicity of Doxil appeared after the third cycle [55].

3. Nanoparticle extravasation and retention in tumors

The second phase of delivery is nanoparticle extravasation from the bloodstream and retention in the tumor tissue. This process is selective for highly permeable tumors that lack lymphatic drainage.

3.1. Tumor vascular permeability and nanoparticle extravasation

Tumor blood vessels are dense, immature, chaotically branched, and dilated [56], and early in cancer research it was observed that large molecules such as proteins were leaking *out* of tumors, suggesting hyperpermeability [57–59]. It was further observed that blood-borne macromolecules >40 kDa and nanoparticles could evade renal clearance and leak *into* tumors [60]. In normal tissues (excepting the RES), the contact layer between blood and tissues is continuous and well sealed against macromolecules and particles [14], preventing extravasation of nanoparticles into most normal tissues with reduced off-target toxicity [1]. This selective extravasation effect favors long-circulating nanoparticles, as this passive targeting effect is an accumulative process. This phenomenon has been observed in both animal and human tumor biology. The earliest example was generated by the Maeda group [2,61–63]: a styrene maleic anhydride polymer was conjugated to neocarzinostatin (SMANCS), and patients treated with this therapeutic were imaged by CT, with tumor accumulation of the therapy reading 10–200 times higher than normal tissues. Harrington et al. [64] demonstrated that ^{111}In-labeled PEGylated liposomes selectively accumulated in the liver, spleen, squamous cell tumor, cardiac blood pool, and bowel using radiographic whole body measurements, confirming the typical BD profile for long-circulating liposomes. Similar radiographic measurements in patients suffering from Kaposi's sarcoma confirmed the selective BD of Doxil [64].

Despite the dramatically improved PK, BD, efficacy and safety profiles of nanomedicines in preclinical models, most of them do not increase overall survival of patients compared to the standard chemotherapy [65]. Patients with HIV-related Kaposi's sarcoma or metastatic breast cancer receiving doxorubicin or Doxil have similar overall survival [66,67]. Similar results were shown for DaunoXome in treating patients with HIV-related Kaposi's sarcoma [68]. Although a couple of positive trials with nanomedicines have been reported, including Doxil for metastatic ovarian cancer [69] and Abraxane for metastatic breast cancer [70], the benefit of nanomedicine in clinical patients has not been consistent. Opaxio exhibited promising efficacy in preclinical models and in a small number of cancer patients in early clinical trials, but failed in phase III trials when the product was tested in a large number of patients [71]. These clinical results suggest that patients have significant variations in tumor pathophysiology, which contributes to the variable therapeutic outcomes, resulting in statistically non-significant results that mask the benefit of nanomedicine. Particularly, heterogeneous tumor vasculature is anticipated to lead to highly variable delivery of nanoparticles [65,72]. Ernsting et al. [73] recently reported that the tumor uptake and efficacy of their nanoparticles were linearly correlated with the tumor blood vessel density ($R^2 > 0.9$). The results suggest that extravasation of nanoparticles is dependent on the tumor vasculature, which has a high degree of variation that results in varying tumor extravasation. It is becoming widely accepted that only a selected population of patients with highly permeable tumors can benefit from nanomedicine [74–76], and a selection tool is needed to identify the receptive population.

3.2. Strategies to enhance the tumor extravasation of nanoparticles

3.2.1. Reduce particle size

Within the systemic circulation phase of drug delivery, the optimal particle size is about 100 nm, evading renal, hepatic and splenic filtration. However, the optimal particle size favoring tumor extravasation is not necessarily equivalent. Cabral et al. [77] compared the accumulation and effectiveness of differently sized long-circulating, drug-loaded polymeric micelles (diameters of 30, 50, 70 and 100 nm). In a hyperpermeable murine colon cancer model, there were no size-dependent restrictions on extravasation in tumors (all tumors exhibited a 10% ID uptake). In contrast, only particles smaller than 50 nm could penetrate poorly permeable hypovascular human pancreatic cancer models, with 30 nm particles fully inhibiting tumor growth and 50 nm particles inhibiting growth by only 50%. Particles above 50 nm had no inhibitory effect in this hypopermeable pancreatic model. Lee et al. [78] showed that accumulation of the 25 and 60 nm particles in the liver and spleen was not significantly different, but tumor uptake of the 25 nm particles was 2-fold higher relative to the 60 nm particles.

3.2.2. Tumor blood vessel modulating treatments

While hyperpermeable, the tortuous and chaotic vasculature of tumors represents a barrier to drug delivery because there is limited perfusion [65,79–81]. The process of angiogenesis is driven by factors released by tumor and stromal cells, and chief among the culprits is VEGF [82]. Blockading VEGF in tumors causes a reduction in the size and diameter of blood vessels with improved blood perfusion, leading to increased delivery of small molecule drugs [83,84]. Vascular normalization may enhance drug delivery for small molecules, but it can actually create barriers to nanomedicine therapy, as normalized blood vessels become less permeable to macromolecules, and the decrease in particle flux across the vessel walls may offset the benefits of increased perfusion [65]. Tanaka et al. [85] demonstrated enhancements to EPR uptake by manipulation of vascular pressures with a prostaglandin analog (Beroprost): prostaglandin caused vasodilation, resulting in thinning of the already deformed tumor capillary wall, which in turn improved extravasation of macromolecules. Seki et al. [86] showed that nitroglycerin enhanced delivery of PEG-conjugated zinc protoporphyrin (PGP) and hence improved therapeutic efficacy *via* sustained EPR effect (more than 24 h). NO_2^- is first liberated from nitroglycerin and is then converted to NO under hypoxic conditions in cancer tissue, resulting in vasodilatation and increased blood flow in the tumor, while NO_2^- production in normal tissue showed no significant increase. Seynhaeve et al. [86] demonstrated that the addition of low-dose tumor necrosis factor-α (TNF-α), which is a pro-inflammatory cytokine with known vascular permeabilizing activity, to systemic injections with PEGylated liposomes augmented tumor accumulation of these liposomes by 5- to 6-fold, which strongly correlated with enhanced tumor response. Seki et al. [87,88] showed that TNF-α can enhance the delivery of viral particles into tumors through a Rho A/Rho kinase dependent mechanism. TNF-α, however, is poorly tolerated when administered systemically, and therefore locoregional setups, such as isolated-limb-perfusion, are needed to exploit their beneficial effects. If such setups are available, the combination of extravasation-enhancing pretreatment with nanomedicine treatment can lead to significant increases in therapeutic efficacy [74]. Kano et al. [89] discovered that pre-treatment with a low dose of a TGF-β inhibitor (LY364947) decreased pericyte coverage of the tumor endothelium, leading to increased vascular permeability to nanoparticles.

Radiation treatment is also known to increase vascular permeability of solid tumors, and enhances the delivery of nanoparticles [90,91]. Li et al. [91] treated an OCa-1 ovarian carcinoma model with 5–15 Gy radiation followed by native paclitaxel and PG-TXL (polyglutamate conjugate of paclitaxel). Radiation significantly elevated VEGF levels, increased tumor vascular permeability by 26%, and improved tumor extravasation of PG-TXL by ~30%, but this result is not found with native paclitaxel. Davies et al. [90] reported similar results in an osteosarcoma xenograft model: they administered Caelyx (liposomal doxorubicin) in control and irradiated mice, and observed improved drug delivery in the irradiated mice and 60–70% efficacy enhancements. They further characterized the tumors with MRI, and demonstrated that radiation treatment enhanced perfusion significantly, an effect independent of drug treatment. Ionizing radiation generates reactive oxygen species (ROS) in DNA, resulting in tissue injury, including endothelial cell damage, with an increase in vascular permeability, edema, and fibrin accumulation in the extracellular matrix [92].

3.3. Factors affecting tumor retention of nanoparticles

Another aspect influencing delivery of nanoparticles is the retention effect arising from impaired or absent lymphatic drainage in tumors. It

has been observed that elongated objects exhibit enhanced tissue retention following extravasation: Park et al. [93] demonstrated that dextran-coated nanochains and spheres (length ~ 50 nm) both extravasated into tumor tissue, but 48 h after injection the spheres had largely returned to the circulation, whereas the injected chains were better retained. Size also impacts retention in the tumor tissue: Torchilin et al. [94] demonstrated that the 10 nm micelles permeated into the tumor within 30 min post-injection, but the dose was not stably retained, with only ¼ of the dose remaining in the tumor in 2 h. When the micelles were labeled with a 2C5 antibody, the tumor retention was significantly improved, with >80% of the dose retaining in the tumor in 2 h. Their data suggests a decreased retention effect for smaller (10 nm) particles, which can be reversed through the use of a targeting ligand.

4. Tumor penetration of nanoparticles and drug release

Nanoparticles that successfully extravasate into tumor tissues face another barrier consisting of high interstitial fluid pressure, dense stromal tissue, and complex interactions with macrophages, fibroblasts, and tumor cells. BD analysis typically involves measurement of gross drug content in tissues, but is increasingly becoming a process of measuring *where* the particles are within tissues. The third phase of drug delivery involves nanoparticle penetration in the tumor tissue and drug release from nanoparticles.

4.1. Tumor physiological factors that impact nanoparticle penetration

4.1.1. Abnormal and heterogeneous vasculature

Tumor vasculature is highly irregular compared to that in normal tissues, with characteristics such as heterogeneous spatial distribution and uneven perfusion and permeability (reviewed in [65]). Tumor periphery is highly perfused, but vascular permeability is lower compared to the hypoxic core, wherein the reverse is observed [95]. Yuan et al. [30] prepared human adenocarcinoma xenografts in a dorsal window chamber model, permitting visualization of tumor vasculature and penetration of labeled liposomes. Compared to normal tissue, the liposomes exhibited significant accumulation in the adenocarcinoma, but did not distribute homogenously: liposomes accumulated in perivascular clusters. Lee at al. [96] compared the intratumoral distribution of ^{111}In labeled polymeric micelles in MCF-7 and MDA-MB-468 tumors using MicroSPECT imaging, demonstrating a similar pattern of heterogeneous distribution. In both studies, nanoparticle uptake occurred mainly in the perfused tumor periphery, suggesting perfusion rather than permeability is the limiting factor for tumor penetration of nanoparticles.

4.1.2. Interstitial fluid pressure (IFP)

While tumor vasculature is often permeable to nanoparticles, further penetration into the tumor tissue depends on convective flow. In normal tissues, there is a net negative pressure drop between the blood vessel and the interstitial space, leading to fluid movement into the interstitial space and ultimately onwards to lymphatic ducts. However, as a result of abnormal permeability, lymphatic vessel malfunction, interstitial fibrosis, contraction of interstitial tissues mediated by stromal fibroblasts [86], and compression from multiplying tumor cells [97], interstitial fluid pressure (IFP) in tumors is increased and can be up to 60 mmHg [86,98–101]. High IFP disrupts normal convective flow, and large molecules and particles that rely on convective flow will not efficiently transport into the tumor compartment [102]. For nanoparticles, extravasation into the tumor periphery may be favored by increased permeability and perfusion, but movement to sites distant from the blood vessels is impaired by high IFP [77,96,103].

4.1.3. Stromal density

Cancer cells are surrounded by basement membrane, fibroblasts, immune cells, and extracellular matrix (ECM), which are collectively termed stroma, and is the dominant fraction of the total tumor mass [104,105]. The interaction between the tumor and stromal cells has been characterized as a wound that does not heal, given the inflammation and matrix building activity [104,106], but unlike normal tissue healing processes, fibroblasts in tumors are unregulated, continuously proliferate, and do not senesce [107]. The extracellular matrix produced by the activated fibroblast is a barrier to convective and diffusive transport, and this is particularly significant for nanoparticles compared to small molecules [106,108,109]. Furthermore, fibroblasts in the stromal tissues generate contractile forces, which increases IFP and reduces perfusion, further inhibiting drug transport and penetration [105]. In studies of nanoparticle penetration, Jain et al. [65] have demonstrated that the dense network of collagen fibers (ECM) prevents intratumoral transport, confining nanoparticles to the perivascular regions of the tumor.

4.1.4. Tumor associated macrophage (TAM)

Tumor tissue is rich in macrophage, with these populations reaching up to 60% of cells in some tumors [110,111]. Tumor associated macrophage (TAM) are well studied in their distinct role in immune suppression, growth promotion, and metastases (refer to review [112]). TAMs have been shown to influence transport and drug release from nanoparticles [113–115]. Opaxio is a polyglutamate-paclitaxel conjugate (PG-TXL), and studies with radiolabeled drug revealed that the drug metabolites were predominantly located within TAMs, whereas level of drug metabolite in tumor cells was 100–1000× less [113]. Furthermore, the intratumoral distribution of PG-DTPA-Gd (a MR contrasted version of the polymer) was overlaid with TAMs, particularly in necrotic area of tumor, suggesting that TAMs were taking up PG and transporting the drug within the tumor [114]. A similar finding on TAM-related biofate was made with IT-101, a cyclodextrin conjugate of camptothecin. In *in vivo* models of glioblastoma, it was shown that microglia (a TAM) and lymphocytes were the predominant cell-types taking up IT-101, with microglia being particularly aggressive on the uptake [115]. Similar to the PG-TXL study, microglia was responsible for transporting the nanoparticles from the periphery into the tumor center within 1 day [71,115].

4.2. Nanoparticle properties that impact the tumor penetration

4.2.1. Size

Lee et al. [78,96] have demonstrated that tumor penetration of the 25-nm particles from the vascular structures into the tumor tissue was doubled compared to the 60-nm particles (20 μm *versus* 46 μm from the nearest blood vessel). Moreover, particles >60 nm in diameter did not penetrate owing to the density of the collagen network [116]. Several studies, however, demonstrated that peak tumor penetration differs for particles with different sizes, and that larger particles can indeed achieve similar tumor penetration as smaller molecules over an extended time frame [78,117].

4.2.2. Zeta potential

Neutral (±10 mV) nanoparticles traveled up to three times more distance than charged analogs, and distributed more homogeneously within tissue: cationic materials tend to interact with negatively charged matrix polymers such as hyaluronan, and anionic materials tend to interact with positively charged matrix such as collagen [118,119], and these interactions impede transport. Nomura et al. [120] determined that liposomes carrying a nearly neutral charge (−2 to −5 mV) were able to penetrate through tumor tissue 14 time more rapidly compared to positively charge liposomes (+48 mV), which barely migrated at all. Similarly, Stylianopoulos et al. [118] demonstrated by modeling and experimental validation that highly positive particles exhibited reduced penetration and distributed less homogenously. Lieleg et al. [119] studied the penetration of charged polystyrene and liposomes in matrix, and found that when the zeta potential was below −20 mV or above 10 mV,

their diffusion coefficients were orders of magnitudes lower than values for neutral particles.

4.2.3. Targeting ligands

Lee et al. [78] showed that the 25 nm EGFR-targeted block copolymer micelles exhibited reduced tumor penetration ($D_{mean} = 29$ μm) compared to the non-targeted micelles ($D_{mean} = 42$ μm) due to the "binding site barrier" effect, where specific binding and/or cellular internalization of antibodies by the targeted cells halts their penetration in solid tumors. This barrier effect was not observed for the 60 nm version of the nanoparticles, as particle penetration was already limited (~20 μm) by matrix interactions related to size.

4.3. Approaches to modulate tumor penetration of therapeutic agents

4.3.1. IFP reduction

Reducing IFP to restore a normalized flow pattern is anticipated to enhance convective transport and intratumoral penetration of therapeutic agents. However, the majority of the studies were performed with small molecules [121,122], and the relevance to nanoparticles is yet to be confirmed. In the first type of approach, tumor vasculature is normalized by treatment with anti-angiogenic drugs which target VEGF, including drugs such as bevacizumab, and cediranib [65,80,123], and which results in lower IFP. In a second approach to IFP reduction, stromal fibroblasts are targeted. Prostaglandins interact with fibroblasts to increase contractile forces and therefore raise IFP. Pietras et al. [124,125] demonstrated that treatment with a prostaglandin inhibitor such as Imatinib reduced IFP and improved small molecule drug delivery within the tumor microenvironment by 1.8-fold. In a third approach, IFP can be reduced by debulking the ECM or stromal cells. Treatment with of ECM with ECM-degrading enzymes such as hyaluronidase or collagenase, or debulking tumors cells with drugs such as paclitaxel can reduce IFP and enhance transport of chemotherapeutics by 4- and 2-fold, respectively [126].

4.3.2. Stromal depletion

There is current interest in targeting stroma with molecules or nanoparticles, and fibroblasts in particular are identified as good targets, to debulk the tumor, reduce tumorigenic stimuli, alleviate high IFP, and restore perfusion and drug delivery [128]. Most recently, Murakami et al. [127] demonstrated that their nanoparticles composed of PEGylated and acetylated carboxymethylcellulose with docetaxel interacted selectively with cancer associated fibroblasts (CAFs) in the breast tumor models (Fig. 4). Greater than 85% of the nanoparticles were internalized by CAFs in the tumor microenvironment possibly *via* an albumin-SPARC (secreted protein acidic and rich is cysteine) dependent mechanism. SPARC is a tissue remodeling molecule produced at high concentrations by tumor stromal cells. This interaction led to almost complete depletion of CAFs within a week, with 70-fold increased tumor perfusion, 50% reduction in ECM and IFP, and >10-fold decrease in metastases. Whether this nanoparticle treatment can increase subsequent delivery of other drugs or macromolecules is yet to be studied. Several approaches to stromal depletion are being tested in clinical trials, including Abraxane (paclitaxel–albumin nanoparticle) and Hedgehog inhibitors [129,130]. In clinical evaluation in combination with gemcitabine, Abraxane (Nab-paclitaxel) reduced pancreatic ECM, possibly due to increased interactions with the stroma cells *via* a SPARC-mediated mechanism. This combination treatment resulted in 3.7-fold increased delivery of gemcitabine into the debulked xenografted tumor [129]. Loeffler et al. [131] showed that fibroblast activation protein (FAP)-vaccinated mice displayed decreased collagen type I expression in the tumor, and as stroma was accordingly less dense, the tumor uptake of doxorubicin was increased up to 70%. They also demonstrated similar effects with fluorescein and albumin, suggesting the stromal depletion strategy may be applied to enhance the delivery of both small molecules and macromolecules.

4.4. Drug release from nanoparticles

As particles extravasate into the tumor, there must be either interstitial drug release, or internalization of the particles and intracellular release to exert pharmacological effects: composition of the nanoparticles must therefore accommodate mechanisms for drug release, preferably sustained release. Two clinical examples (Doxil and SPI-077) illustrate the challenge associated with excessive stability. Doxil delivers 10 to 15 times more doxorubicin to the tumor compared to standard therapy, but Doxil in the tumor has low bioavailability (40–50%) due to slow release, and as a result, efficacy enhancements are modest [132–134]. Similarly, SPI-077 (a liposomal formulation of cisplatin) exhibited significant tumor accumulation but no antitumor effect. Analysis revealed that cisplatin is membrane impermeable, and was retained inside the stable liposomes and not bioavailable [132,135].

Conversely, a formulation can exhibit excessive instability, and in the field of taxane therapies, this is a persistent challenge. Taxanes have been formulated into polymeric micelles such as Genexol [136] and NK105 [137], and while these technologies enhance efficacy, the taxanes rapidly partition out of the polymeric micelles and bind with serum proteins during blood circulation, and the PK improvement over the standard formulations (Taxol or Taxotere) is not significant in human patients [136,138,139]. In the Abraxane formulation, human serum albumin is complexed with paclitaxel to form 130-nm particles, and likewise, while efficacy enhancements are observed due to an increase in the tolerated dose, the PK profile of the paclitaxel is unchanged [70,140–142]. Opaxio is a conjugate of paclitaxel and polyglutamate, and while positive results in Phase I and II were reported and PK parameters were significantly enhanced [143], the hallmark taxane side effects of neutropenia persisted, and it failed to enhance efficacy in Phase III. In preclinical evaluation it was observed that Opaxio decomposed during circulation, forming polymeric fragments of taxane that distributed to many normal organs to a significant extent [144]. It may be that Opaxio is not stable enough to minimize toxicity and leverage the EPR effect to the full advantage. The challenge then is to maintain stability to achieve improved PK profiles, while providing for a release mechanism inside the tumor.

4.5. Factors impacting cellular internalization of nanoparticles and the drug release

4.5.1. Mechanisms of cellular internalization of nanoparticles

There are two major endocytic mechanisms by which cells take up particles and macromolecules, and these are referred to as phagocytosis and pinocytosis [145]. Large particles (>1 μm) are generally internalized by phagocytosis mechanisms, which are present only on professional phagocytic cells, such as macrophages, neutrophils, or dendritic cells [146]. Therefore pinocytosis is more relevant to cellular uptake of nanoparticles and can occur either *via* adsorptive pinocytosis or *via* receptor-mediated endocytosis [147]. Pinocytic mechanisms of uptake can be further divided into caveolae-mediated endocytosis (~60 nm) or clathrin-mediated endocytosis (~120 nm), as well as clathrin-independent or caveolin-independent endocytosis (~90 nm) [146]. The details of the exact mode of endocytosis are important because they determine the path of trafficking through various possible subcellular compartments. For example, nanoparticles internalized through clathrin-mediated endocytosis are destined for a lysosomal compartment, whereas those internalized through a caveolin-mediated process are not. In clathrin-mediated endocytosis internalization, endosomal escape must occur before fusion with a lysosome to prevent degradation of the cargo under harsh lysosomal conditions. In either case, endosomal escape is usually necessary to allow access of the carrier to the desired subcellular compartment. Ligands such as folic acid, albumin and cholesterol conjugated to the surface of engineered nanoparticles can facilitate uptake through caveolin-mediated endocytosis, whereas ligands for glycoreceptors promote clathrin-mediated endocytosis. Alternatively,

macropinocytosis, a non-caveolin-mediated, non-clathrin-mediated process, can be engaged by incorporating cell-penetrating peptides, such as a trans-activating transcriptional activator (TaT) peptide into the design of engineered nanoparticles. For a nanoparticle entering the lysosomal compartments, drug release can be engineered to occur *via* hydrolysis of sensitive functional groups (such as an ester): the released drug must be reasonably resistant to the lysosomal environment and be able to escape into the cytosol [148–150].

4.5.2. Size

Nanoparticle size is a key parameter affecting the cellular uptake rate as it influences their internalization mechanism. In general, particles in the 40–200 nm range exhibit cellular uptake *in vitro* [151,152]. Gratton et al. [152] examined the uptake of hydrogel particles ranging from 1 to 200 nm in diameter in HeLa cells, and found that very small (1 nm) and larger (150–200 nm) particles were readily internalized. Jiang et al. [153] investigated the size-dependent binding and uptake of the transtuzumab-conjugated nanoparticles (2–100 nm) with ErbB2+ cells and found that 40–50 nm particles exhibited the highest amount of cellular internalization, which may be due to the optimal antibody density on the particle surface that triggers maximal cross-linking of the membrane receptors.

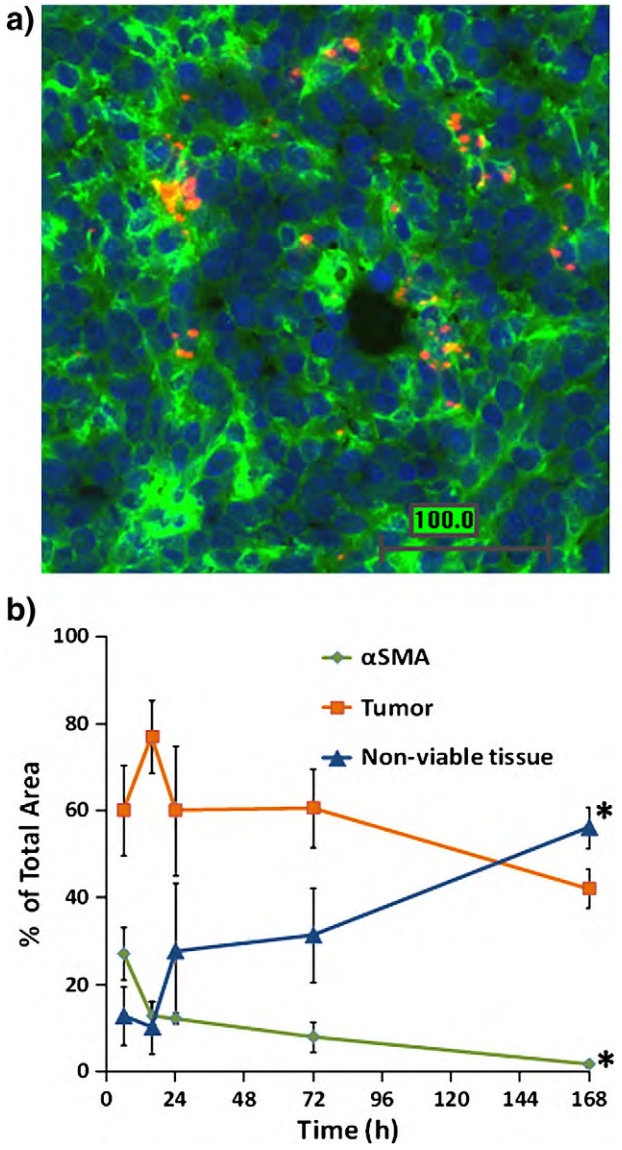

Fig. 4. Cellax nanoparticles target cancer-associated fibroblasts. (a) Balb/c mice bearing 4T1 breast tumors were treated with fluorescently labeled Cellax particles (red), and α-SMA+ CAF were immunostained with FITC (green). Definiens image analysis of tumors for total area (defined by DAPI nuclear staining), α-SMA content (green) and Cellax-DiI (red) demonstrated that 85% of the Cellax particles were associated with α-SMA+ CAF. Cellax-treated 4T1 tumors were analyzed to quantify different cell populations in the tumors over a time course (b): subsequent to therapy, α-SMA content dropped rapidly over 16 h, followed by a steady decrease over 168 h. Tumor cells as a percentage of total tumor area did not undergo a significant decline in the 168 h timeframe, whereas non-viable tissue increased significantly, suggesting that the decline of α-SMA+ cells is the primary therapeutic effect. Adapted from ref [127].

4.5.3. Shape

Gratton et al. [152] designed a series of cationic cross-linked PEG-based hydrogels of varying sizes and shapes *via* a top-down lithographic fabrication method (PRINT: Particle Replication In Non-wetting Templates) and examined the cellular internalization pathways using Hela cells. Nonspherical particles with dimensions as large as 3 μm were easily internalized by using several different mechanisms of endocytosis. Similar findings demonstrate the enhanced internalization of nonspherical particles over their spherical counterparts for nanosized rod-like biodegradable mesoporous silica nanoparticles [154] and iron oxide nanoworms [93]. On the contrary, several other studies have found that the spherical forms of gold nanoparicles [155] and polymeric nanoparticles [156] were internalized to a greater extent than their corresponding nonspherical particles. For example, cells took up 5 and 4-fold more 74 and 14 nm spherical gold nanoparticles than 74 × 14 nm rod-shaped gold nanoparticles, respectively [155]. Nevertheless, shape of particles not only affects tumor cell internalization but also determines the interaction with RES, and the PK and tumor retention as discussed in the previous sections. Impacts of shape in the three phases of delivery should be comprehensively considered when designing nanoparticles.

4.5.4. PEGylation

To reduce opsonization by blood proteins and clearance by RES, hydrophilic stealth polymers (e.g., PEG) have been used as a surface coating material. PEG, however, may be an obstacle and hinder to interaction with target cells, resulting in reduced efficacy. Several different approaches have been made to remove the PEG coating after the particle arrives at the target site. Guo et al. [157] prepared a removable PEG coating which stabilizes the fusogenic DOPE in liposomes at neutral pH. PEG was linked to DOPE *via* a diorthoester bond, and hydrolysis of the conjugation at the low endosomal pH in the range of 5–6 occurred within 1 h, leading to particle fusion with the endosomal membrane and release of contents into the cytosol. A similar strategy was applied to TAT-liposomes masked with a cleavable PEG coating: the PEG chains were released at the acidic pH (pH 5–6), exposing the TAT peptides to interact and enhance internalization by the targeted cancer cells [158]. Similarly, the same group shielded the TAT-liposomes with a long-chain PEG, which was conjugated to the liposomal surface *via* a MMP2 cleavable peptide (Gly-Pro-Leu-Gly-Ile-Ala-Gly-Gln) [159]. They reported that the liposomes were de-PEGylated by the extracellular MMP2 in the tumor cells, exposing the TAT peptide on the nanoparticle surface for increased cellular uptake. Maclachlan's group [160] developed stabilized nucleic acid lipid particles (SNALP) consisting of a siRNA encapsulated in an ionizable lipid bilayer (pKa ~6) with a PEGylated lipid. They found that when the carbon chain length of the PEGylated lipid was shortened from C20 to C14, the blood circulation time was decreased, but accompanied with increased hepatocellular uptake of the formulation, enhanced gene silencing activity in the liver, and reduced cytokine stimulation. The PEGylated lipid with a shortened carbon chain is diffusive, and readily leaves the lipid bilayer during blood circulation to facilitate binding of Apo E to the naked SNALP, which in turn recognizes Apo E and LDL receptors on the hepatocytes, therefore triggering endocytosis. In the acidic endosomal and lysosomal environment, SNALP is ionized and becomes cationic to interact with the negatively charged lipid membrane, promoting siRNA to escape into the cytosol, the site of action. On the other hand, SNALP prepared with long acyl chain PEGylated

lipids remain stable in the blood circulation, and have an increased probability of interacting with immune cells, inducing enhanced proinflammatory cytokine production.

4.5.5. Zeta potential

Cationic nanoparticles are generally known to exhibit increased uptake by cells *via* the charge–charge interaction mediated adsorptive endocytosis compared to neutral and anionic particles [161–163]. Again, the PK of the charged nanoparticle has to be considered, as charged nanoparticles often display increased interaction with serum proteins, resulting in accelerated blood clearance compared to neutral particles. As just discussed, it is feasible to design nanoparticles that shed PEG-shielding after tumor extravasation in order to expose cationic particles that can interact with target cells [164,165]. In a slightly different variant of this approach, Choi et al. [166] formulated poly(ethyleneglycol)-diorthoester-distearoylglycerol lipid (POD) stabilized plasma lipid nanoparticles (SPLP): POD-SPLP contain 13 wt.% PEG: the PEG brush dissipated at pH 5.3 within 110 min, exposing a cationic particle. Both the POD-SPLP and PEG-SPLP were internalized to a qualitatively similar extent within 2 h of incubation but gene transfer increased up to 3 orders of magnitude with POD-SPLP, due to more rapid escape of plasmid DNA from the endosome.

4.5.6. Targeting ligands

A commonly used strategy for improving bioavailability of nanoparticles in a tumor is to conjugate a targeting ligand, allowing the binding with the surface receptor on the tumor cells, triggering receptor-mediated endocytosis for increased intracellular delivery of a drug. Although success has been reported for many nanoparticle systems and animal models, this approach suffers from the following disadvantages: first, cellular internalization happens only after extravasation of nanoparticles, and the cellular uptake only occurs around the microvessels, resulting in limited tumor penetration and heterogeneous drug uptake [3]. As discussed earlier, Lee et al. [78] demonstrated that the targeted nanoparticles display restricted penetration compared to non-targeted particles; second, some ligand-conjugated nanoparticles, including antibody- [167] or small molecule-decorated nanoparticles [168,169] display enhanced blood clearance, reducing the tumor accumulation; third, cellular internalization by receptor-mediated endocytosis leads to drug decomposition in the endosome/lysosome [170]. Therefore, targeted nanoparticles do not always exhibit improved therapy compared to the non-targeted ones [132].

Another important point to note is that conjugating a tumor-selective ligand onto nanoparticles does not improve the specificity of tissue distribution, which is mainly determined by nanoparticle physicochemical properties, and the ligand only sees the antigen after nanoparticle extravasation. Using proton emission tomography/computed tomography (PET/CT), Bartlett et al. [171,172] compared the biological activity of siRNA payloads in tumors delivered *via* non-targeted and transferrin conjugated nanoparticles. They found no difference in BD between the targeted and the non-targeted nanocomplexes, while increased gene silencing activity was seen with the targeted complex. The authors concluded that the primary function of the ligand was not in targeting the complexes to the tumor tissue, but to increase the intracellular uptake. Similar results have been reported by other groups [167,173].

4.5.7. TAM content and drug release

Zamboni et al. [174] have shown that drug release of a camptothecin analog from the PEGylated liposomes was more efficient in tumors characterized by higher macrophage content. For example: 4.9 ± 3.0% of SKOV-3 tumors stained positive for TAM, whereas only 1.1 ± 0.7% in A375 tumor. While the total drug accumulation in the tumor tissues was similar (13–16 μg/mL h), release of camptothecin in the extracellular fluid was 2-fold higher in the TAM-rich SKOV-3 tumors. The data suggest that TAM not only is active in phagocytosing nanoparticles, but also efficient in digesting nanoparticles and facilitating drug release. However, whether TAM content can be a biomarker to correlate drug release from nanoparticles and their efficacy needs to be validated.

5. Conclusion and perspectives

There is a continuum of biological barriers to effective drug delivery by nanoparticles (Fig. 1), ranging from the RES interaction with nanoparticles, to the extravasation of nanoparticles into highly permeable tumor tissues, and penetration of nanoparticles through the stroma and ultimate drug release around or inside the target cells. There are conflicting design parameters as a result of this multi-system interaction, especially in optimal size. Approved cancer nanomedicines (Doxil, DaunoXome, Abraxane and Marqibo) are 80–130 nm in diameter. However, there is increasing interest in developing small particles (<50 nm) exhibiting improved tumor permeability and penetration.

PEGylation has been employed in many nanoparticles to reduce the RES interaction and prolong the blood circulation. Nevertheless, the RES is still responsible for clearing majority of nanoparticles, typically leaving <10% ID/g delivered to the tumors [3,132]. There are limits to how much PEG can be integrated into a nanoparticle before it destabilizes the structure. The Huang lab [175,176] has demonstrated in their LPD (lipid-polycation-DNA) and LCP (lipid-calcium phosphate) nanoparticle systems that >10 mol% of DSPE-PEG_{2000} could be introduced to the lipid membranes that are stabilized by charge–charge interaction. These highly PEGylated LPD and LCP nanoparticles displayed minimal RES clearance in the liver (~10% ID), a clear differentiation from many other nanoparticles. However, PEGylation has been shown to reduce nanoparticle interaction with target cells, and is responsible for immune response, especially when an immunostimulatory agent is carried, such as pDNA and siRNA. A variety of strategies have been developed to facilitate de-PEGylation of nanoparticles to reduce the immunotoxicity or cellular bioavailability. Developing a PEG alternative to shield nanoparticles from RES recognition remains an open challenge.

Clinical tumors possess a high degree of variation in vasculature, which impacts nanoparticle extravasation and the intratumoral distribution, leading to varying therapeutic activities among patients [75,76]. Patient characteristics (e.g., age, gender, tumor type, tumor location, body composition and prior treatments) can also affect the EPR effect of nanomedicine [177]. Additionally, the EPR effect is mainly observed with large solid tumors, and whether this effect applies to small metastases needs to be validated in a large number of patients. To improve therapeutic outcomes, a selection tool needs to be developed to stratify patients into candidates and non-candidates for nanomedicine therapy. A nanoparticle can be manufactured with multiple functions, delivering both drug and imaging agents, enabling real-time and non-invasive measurement of PK, BD and tumor delivery of the nanoparticles. In future, cancer patients could then be screened for treatment suitability using multifunctional nanoparticles and the corresponding imaging technologies. Karathanasis et al. [178] screened mouse breast cancer models with an injectable liposomal probe containing iodine to identify which subgroups were good candidates for nanoparticle therapy, and demonstrated excellent correlation ($R^2 = 0.838$) between SPECT measurements and therapeutic response to the liposomal doxorubicin. Ideally, a general method utilizing a contrast agent and MRI can be developed to screen the prevalence of the EPR effect in human tumors and to stratify patients for receiving nanotherapeutics.

The issue of low drug bioavailability exemplified by Doxil and SPI-077 (PEGylated liposomal cisplatin) is a significant concern in the design of nanoparticles. The development of triggered-release nanoparticles, which release drug locally in the tumor, achieves improved bioavailability while reducing systemic exposure. The most advanced triggered release technology is the hyperthermia-activated liposomal formulation, a nanoparticle that burst-releases 100% drug content at 41–42 °C within 20 s, but is relatively stable at 37 °C [179–183]. In combination with image-guided heating technologies, the drug can be released intravascularly

within the locally heated tumor, generating a high drug concentration gradient for improved delivery and tumor penetration of bioavailable drug. This EPR-effect-independent nanotechnology is being tested in clinical trials. The design of nanoparticles capable of controlled release in the tumor compartment remains an area of pursuit in the field [148–150]. It is also suggested that more research should be directed towards development of new types of nanoparticle delivery systems that do not rely on the EPR effect.

While ligand targeted therapies are experiencing some success, an effective interaction between a ligand and the tumor cell can occur only after the targeted nanoparticles have evaded the RES clearance, extravasated into the tumor tissue and penetrated through the ECM and stroma [65,78]. Due to the difficulty in targeting tumor cells, specific receptors on endothelium within tumors are attractive targets as they present to the bloodstream and circulating nanoparticles [184]. The most commonly utilized ligand is RGD, a peptide recognized by integrins overexpressed on angiogenic endothelial cells [116]. Recently, the Ruoslahti group [118] developed a tumor penetrating peptide, iRGD (CRGDK/RGPD/EC): iRGD targets the integrins on tumor vascular endothelial cells with the RGD motif, and then the peptide is digested to expose RGDK/R, which binds to NRP-1 and induces vascular and tissue permeabilization. Conjugation or co-injection of iRGD with a macromolecule significantly improved the tumor delivery by >7-fold.

In the past few decades, the nanomedicine research has been focused on optimizing the physicochemical parameters of nanoparticles (size, shape, surface charge, ligand, release rate) to obtain optimal PK and delivery. Current research is emphasizing on improving understanding of how human physiology and tumor biology affect PK, BD and intratumoral penetration of nanoparticles. Various approaches have been investigated to modulate the tumor microenvironment to allow increased extravasation of nanoparticles, including modulating the vascular dynamics (blood flow, pressure and permeability), and debulking the tumor by depleting the stromal component (CAFs, ECM). It is now believed that both optimization of the nanoparticles and the tumor microenvironment are required for optimal delivery [75]. Currently, the field of research is still focused on addressing the permeability part of the EPR equation with less emphasis on the retention aspect, which is driven by the impaired lymphatic drainage in the tumor. More functional imaging technologies with quantitative capabilities should be developed to study the lymphatic function in the tumor, and how this parameter impacts IFP, nanoparticle penetration and retention. With gains in fundamental knowledge, rational design of an optimal nanomedicine can then be realized to achieve the maximized therapeutic effect in image-stratified patients.

Acknowledgment

The authors acknowledge the following funding agencies: the Ontario Institute for Cancer Research, MaRS Innovation, the Ontario Centres of Excellence, the Canadian Institutes of Health Research, the Prostate Cancer Foundation, and the National Institutes of Health.

References

[1] J. Fang, H. Nakamura, H. Maeda, The EPR effect: unique features of tumor blood vessels for drug delivery, factors involved, and limitations and augmentation of the effect, Adv. Drug Deliv. Rev. 63 (2011) 136–151.
[2] J. Fang, T. Sawa, H. Maeda, Factors and mechanism of "EPR" effect and the enhanced antitumor effects of macromolecular drugs including SMANCS, Adv. Exp. Med. Biol. 519 (2003) 29–49.
[3] S.D. Li, L. Huang, Pharmacokinetics and biodistribution of nanoparticles, Mol. Pharm. 5 (2008) 496–504.
[4] D. Liu, A. Mori, L. Huang, Role of liposome size and RES blockade in controlling biodistribution and tumor uptake of GM1-containing liposomes, Biochim. Biophys. Acta 1104 (1992) 95–101.
[5] S.M. Moghimi, A.C. Hunter, Capture of stealth nanoparticles by the body's defences, Crit. Rev. Ther. Drug Carrier Syst. 18 (2001) 527–550.
[6] P. Opanasopit, M. Nishikawa, M. Hashida, Factors affecting drug and gene delivery: effects of interaction with blood components, Crit. Rev. Ther. Drug Carrier Syst. 19 (2002) 191–233.
[7] S. Nagayama, K. Ogawara, Y. Fukuoka, K. Higaki, T. Kimura, Time-dependent changes in opsonin amount associated on nanoparticles alter their hepatic uptake characteristics, Int. J. Pharm. 342 (2007) 215–221.
[8] H. Otsuka, Y. Nagasaki, K. Kataoka, PEGylated nanoparticles for biological and pharmaceutical applications, Adv. Drug Deliv. Rev. 55 (2003) 403–419.
[9] Y. Sadzuka, S. Hirotsu, S. Hirota, Effect of liposomalization on the antitumor activity, side-effects and tissue distribution of CPT-11, Cancer Lett. 127 (1998) 99–106.
[10] P. Crosasso, M. Ceruti, P. Brusa, S. Arpicco, F. Dosio, L. Cattel, Preparation, characterization and properties of sterically stabilized paclitaxel-containing liposomes, J. Control. Release 63 (2000) 19–30.
[11] W.L. Lu, X.R. Qi, Q. Zhang, R.Y. Li, G.L. Wang, R.J. Zhang, S.L. Wei, A pegylated liposomal platform: pharmacokinetics, pharmacodynamics, and toxicity in mice using doxorubicin as a model drug, J. Pharmacol. Sci. 95 (2004) 381–389.
[12] D.E. Owens III, N.A. Peppas, Opsonization, biodistribution, and pharmacokinetics of polymeric nanoparticles, Int. J. Pharm. 307 (2006) 93–102.
[13] S.D. Perrault, C. Walkey, T. Jennings, H.C. Fischer, W.C. Chan, Mediating tumor targeting efficiency of nanoparticles through design, Nano Lett. 9 (2009) 1909–1915.
[14] F. Alexis, E. Pridgen, L.K. Molnar, O.C. Farokhzad, Factors affecting the clearance and biodistribution of polymeric nanoparticles, Mol. Pharm. 5 (2008) 505–515.
[15] C. Fang, B. Shi, Y.Y. Pei, M.H. Hong, J. Wu, H.Z. Chen, *In vivo* tumor targeting of tumor necrosis factor-alpha-loaded stealth nanoparticles: effect of MePEG molecular weight and particle size, Eur. J. Pharm. Sci. 27 (2006) 27–36.
[16] M.J. Ernsting, W.L. Tang, N.W. Maccallum, S.D. Li, Preclinical pharmacokinetic, biodistribution, and anti-cancer efficacy studies of a docetaxel–carboxymethylcellulose nanoparticle in mouse models, Biomaterials 33 (2012) 1445–1454.
[17] C.D. Walkey, J.B. Olsen, H. Guo, A. Emili, W.C. Chan, Nanoparticle size and surface chemistry determine serum protein adsorption and macrophage uptake, J. Am. Chem. Soc. 134 (2012) 2139–2147.
[18] N. Dos Santos, C. Allen, A.M. Doppen, M. Anantha, K.A. Cox, R.C. Gallagher, G. Karlsson, K. Edwards, G. Kenner, L. Samuels, M.S. Webb, M.B. Bally, Influence of poly(ethylene glycol) grafting density and polymer length on liposomes: relating plasma circulation lifetimes to protein binding, Biochim. Biophys. Acta 1768 (2007) 1367–1377.
[19] A. Chanan-Khan, J. Szebeni, S. Savay, L. Liebes, N.M. Rafique, C.R. Alving, F.M. Muggia, Complement activation following first exposure to pegylated liposomal doxorubicin (Doxil): possible role in hypersensitivity reactions, Ann. Oncol. 14 (2003) 1430–1437.
[20] J. Szebeni, Complement activation-related pseudoallergy: a new class of drug-induced acute immune toxicity, Toxicology 216 (2005) 106–121.
[21] W.C. Chen, J.P. May, S.D. Li, Immune responses of therapeutic lipid nanoparticles, Nanotechnol. Rev. 2 (2013) 201–213.
[22] T. Ishida, T. Ichikawa, M. Ichihara, Y. Sadzuka, H. Kiwada, Effect of the physicochemical properties of initially injected liposomes on the clearance of subsequently injected PEGylated liposomes in mice, J. Control. Release 95 (2004) 403–412.
[23] A. Judge, K. McClintock, J.R. Phelps, I. Maclachlan, Hypersensitivity and loss of disease site targeting caused by antibody responses to PEGylated liposomes, Mol. Ther. 13 (2006) 328–337.
[24] M. Barz, R. Luxenhofer, R. Zentel, M.J. Vicent, Overcoming the PEG-addiction: well-defined alternatives to PEG, from structure–property relationships to better defined therapeutics, Polym. Chem. 2 (2011) 1900–1918.
[25] R. Hoogenboom, Poly(2-oxazoline)s: a polymer class with numerous potential applications, Angew. Chem. Int. Ed. Engl. 48 (2009) 7978–7994.
[26] M. Nahrendorf, E. Keliher, B. Marinelli, P. Waterman, P.F. Feruglio, L. Fexon, M. Pivovarov, F.K. Swirski, M.J. Pittet, C. Vinegoni, R. Weissleder, Hybrid PET-optical imaging using targeted probes, Proc. Natl. Acad. Sci. U. S. A. 107 (2010) 7910–7915.
[27] C.H. Choi, C.A. Alabi, P. Webster, M.E. Davis, Mechanism of active targeting in solid tumors with transferrin-containing gold nanoparticles, Proc. Natl. Acad. Sci. U. S. A. 107 (2010) 1235–1240.
[28] P.L. Rodriguez, T. Harada, D.A. Christian, D.A. Pantano, R.K. Tsai, D.E. Discher, Minimal "Self" peptides that inhibit phagocytic clearance and enhance delivery of nanoparticles, Science 339 (2013) 971–975.
[29] H.S. Choi, W. Liu, P. Misra, E. Tanaka, J.P. Zimmer, B. Itty Ipe, M.G. Bawendi, J.V. Frangioni, Renal clearance of quantum dots, Nat. Biotechnol. 25 (2007) 1165–1170.
[30] F. Yuan, M. Dellian, D. Fukumura, M. Leunig, D.A. Berk, V.P. Torchilin, R.K. Jain, Vascular permeability in a human tumor xenograft: molecular size dependence and cutoff size, Cancer Res. 55 (1995) 3752–3756.
[31] L.T. Chen, L. Weiss, The role of the sinus wall in the passage of erythrocytes through the spleen, Blood 41 (1973) 529–537.
[32] S.M. Moghimi, A.C. Hunter, J.C. Murray, Long-circulating and target-specific nanoparticles: theory to practice, Pharmacol. Rev. 53 (2001) 283–318.
[33] J. Hrkach, D. Von Hoff, M.M. Ali, E. Andrianova, J. Auer, T. Campbell, D. De Witt, M. Figa, M. Figueiredo, A. Horhota, S. Low, K. McDonnell, E. Peeke, B. Retnarajan, A. Sabnis, E. Schnipper, J.J. Song, Y.H. Song, J. Summa, D. Tompsett, G. Troiano, T. Van Geen Hoven, J. Wright, P. Lorusso, P.W. Kantoff, N.H. Bander, C. Sweeney, O.C. Farokhzad, R. Langer, S. Zale, Preclinical development and clinical translation of a PSMA-targeted docetaxel nanoparticle with a differentiated pharmacological profile, Sci. Transl. Med. 4 (2012) 128ra139.
[34] J.A. Champion, S. Mitragotri, Role of target geometry in phagocytosis, Proc. Natl. Acad. Sci. U. S. A. 103 (2006) 4930–4934.
[35] J.A. Champion, S. Mitragotri, Shape induced inhibition of phagocytosis of polymer particles, Pharm. Res. 26 (2009) 244–249.

[36] Y. Geng, P. Dalhaimer, S. Cai, R. Tsai, M. Tewari, T. Minko, D.E. Discher, Shape effects of filaments *versus* spherical particles in flow and drug delivery, Nat. Nanotechnol. 2 (2007) 249–255.
[37] S. Li, J. Nickels, A.F. Palmer, Liposome-encapsulated actin-hemoglobin (LEAcHb) artificial blood substitutes, Biomaterials 26 (2005) 3759–3769.
[38] T. Cedervall, I. Lynch, M. Foy, T. Berggard, S.C. Donnelly, G. Cagney, S. Linse, K.A. Dawson, Detailed identification of plasma proteins adsorbed on copolymer nanoparticles, Angew. Chem. Int. Ed. Engl. 46 (2007) 5754–5756.
[39] A. Gessner, R. Waicz, A. Lieske, B. Paulke, K. Mader, R.H. Muller, Nanoparticles with decreasing surface hydrophobicities: influence on plasma protein adsorption, Int. J. Pharm. 196 (2000) 245–249.
[40] P.R. Cullis, A. Chonn, S.C. Semple, Interactions of liposomes and lipid-based carrier systems with blood proteins: relation to clearance behaviour *in vivo*, Adv. Drug Deliv. Rev. 32 (1998) 3–17.
[41] A. Chonn, S.C. Semple, P.R. Cullis, Association of blood proteins with large unilamellar liposomes *in vivo*. Relation to circulation lifetimes, J. Biol. Chem. 267 (1992) 18759–18765.
[42] S.M. Moghimi, H.M. Patel, Tissue specific opsonins for phagocytic cells and their different affinity for cholesterol-rich liposomes, FEBS Lett. 233 (1988) 143–147.
[43] J. Senior, J.C. Crawley, G. Gregoriadis, Tissue distribution of liposomes exhibiting long half-lives in the circulation after intravenous injection, Biochim. Biophys. Acta 839 (1985) 1–8.
[44] T.M. Allen, C. Hansen, Pharmacokinetics of stealth *versus* conventional liposomes: effect of dose, Biochim. Biophys. Acta 1068 (1991) 133–141.
[45] D.C. Drummond, O. Meyer, K. Hong, D.B. Kirpotin, D. Papahadjopoulos, Optimizing liposomes for delivery of chemotherapeutic agents to solid tumors, Pharmacol. Rev. 51 (1999) 691–743.
[46] K. Xiao, Y. Li, J. Luo, J.S. Lee, W. Xiao, A.M. Gonik, R.G. Agarwal, K.S. Lam, The effect of surface charge on *in vivo* biodistribution of PEG-oligocholic acid based micellar nanoparticles, Biomaterials 32 (2011) 3435–3446.
[47] T.S. Levchenko, R. Rammohan, A.N. Lukyanov, K.R. Whiteman, V.P. Torchilin, Liposome clearance in mice: the effect of a separate and combined presence of surface charge and polymer coating, Int. J. Pharm. 240 (2002) 95–102.
[48] A. Gessner, A. Lieske, B. Paulke, R. Muller, Influence of surface charge density on protein adsorption on polymeric nanoparticles: analysis by two-dimensional electrophoresis, Eur. J. Pharm. Biopharm. 54 (2002) 165–170.
[49] A. Gessner, A. Lieske, B.R. Paulke, R.H. Muller, Functional groups on polystyrene model nanoparticles: influence on protein adsorption, J. Biomed. Mater. Res. A 65 (2003) 319–326.
[50] J.S. Zhang, F. Liu, L. Huang, Implications of pharmacokinetic behavior of lipoplex for its inflammatory toxicity, Adv. Drug Deliv. Rev. 57 (2005) 689–698.
[51] W. Li, F.C. Szoka Jr., Lipid-based nanoparticles for nucleic acid delivery, Pharm. Res. 24 (2007) 438–449.
[52] M. Wang, M. Thanou, Targeting nanoparticles to cancer, Pharmacol. Res. 62 (2010) 90–99.
[53] N.M. La-Beck, B.A. Zamboni, A. Gabizon, H. Schmeeda, M. Amantea, P.A. Gehrig, W.C. Zamboni, Factors affecting the pharmacokinetics of pegylated liposomal doxorubicin in patients, Cancer Chemother. Pharmacol. 69 (1) (2012) 43–50.
[54] H. Wu, R.K. Ramanathan, B.A. Zamboni, S. Strychor, S. Ramalingam, R.P. Edwards, D.M. Friedland, R.G. Stoller, C.P. Belani, L.J. Maruca, Y.J. Bang, W.C. Zamboni, Mechanism-based model characterizing bidirectional interaction between PEGylated liposomal CKD-602 (S-CKD602) and monocytes in cancer patients, Int. J. Nanomedicine 7 (2012) 5555–5564.
[55] A. Gabizon, R. Isacson, O. Rosengarten, D. Tzemach, H. Shmeeda, R. Sapir, An open-label study to evaluate dose and cycle dependence of the pharmacokinetics of pegylated liposomal doxorubicin, Cancer Chemother. Pharmacol. 61 (2008) 695–702.
[56] W. Lewis, The vascular pattern of tumors, Bull. Johns Hopkins Hosp. 41 (1927) 156–162.
[57] J.C. Underwood, I. Carr, The ultrastructure and permeability characteristics of the blood vessels of a transplantable rat sarcoma, J. Pathol. 107 (1972) 157–166.
[58] H.I. Peterson, K.L. Appelgren, Experimental studies on the uptake and rentention of labelled proteins in a rat tumour, Eur. J. Cancer 9 (1973) 543–547.
[59] L.E. Gerlowski, R.K. Jain, Microvascular permeability of normal and neoplastic tissues, Microvasc. Res. 31 (1986) 288–305.
[60] H. Maeda, J. Takeshita, R. Kanamaru, A lipophilic derivative of neocarzinostatin. A polymer conjugation of an antitumor protein antibiotic, Int. J. Pept. Protein Res. 14 (1979) 81–87.
[61] T. Konno, H. Maeda, K. Iwai, S. Maki, S. Tashiro, M. Uchida, Y. Miyauchi, Selective targeting of anti-cancer drug and simultaneous image enhancement in solid tumors by arterially administered lipid contrast medium, Cancer 54 (1984) 2367–2374.
[62] H. Maeda, T. Sawa, T. Konno, Mechanism of tumor-targeted delivery of macromolecular drugs, including the EPR effect in solid tumor and clinical overview of the prototype polymeric drug SMANCS, J. Control. Release 74 (2001) 47–61.
[63] H. Maeda, H. Nakamura, J. Fang, The EPR effect for macromolecular drug delivery to solid tumors: improvement of tumor uptake, lowering of systemic toxicity, and distinct tumor imaging *in vivo*, Adv. Drug Deliv. Rev. 65 (2013) 71–79.
[64] K.J. Harrington, S. Mohammadtaghi, P.S. Uster, D. Glass, A.M. Peters, R.G. Vile, J.S. Stewart, Effective targeting of solid tumors in patients with locally advanced cancers by radiolabeled pegylated liposomes, Clin. Cancer Res. 7 (2001) 243–254.
[65] R.K. Jain, T. Stylianopoulos, Delivering nanomedicine to solid tumors, Nat. Rev. Clin. Oncol. 7 (2010) 653–664.
[66] D.W. Northfelt, B.J. Dezube, J.A. Thommes, B.J. Miller, M.A. Fischl, A. Friedman-Kien, L.D. Kaplan, C.Du. Mond, R.D. Mamelok, D.H. Henry, Pegylated-liposomal doxorubicin *versus* doxorubicin, bleomycin, and vincristine in the treatment of AIDS-related Kaposi's sarcoma: results of a randomized phase III clinical trial, J. Clin. Oncol. 16 (1998) 2445–2451.
[67] M.E. O'Brien, N. Wigler, M. Inbar, R. Rosso, E. Grischke, A. Santoro, R. Catane, D.G. Kieback, P. Tomczak, S.P. Ackland, F. Orlandi, L. Mellars, L. Alland, C. Tendler, Reduced cardiotoxicity and comparable efficacy in a phase III trial of pegylated liposomal doxorubicin HCl (CAELYX/Doxil) *versus* conventional doxorubicin for first-line treatment of metastatic breast cancer, Ann. Oncol. 15 (2004) 440–449.
[68] P.S. Gill, J. Wernz, D.T. Scadden, P. Cohen, G.M. Mukwaya, J.H. von Roenn, M. Jacobs, S. Kempin, I. Silverberg, G. Gonzales, M.U. Rarick, A.M. Myers, F. Shepherd, C. Sawka, M.C. Pike, M.E. Ross, Randomized phase III trial of liposomal daunorubicin *versus* doxorubicin, bleomycin, and vincristine in AIDS-related Kaposi's sarcoma, J. Clin. Oncol. 14 (1996) 2353–2364.
[69] A.N. Gordon, J.T. Fleagle, D. Guthrie, D.E. Parkin, M.E. Gore, A.J. Lacave, Recurrent epithelial ovarian carcinoma: a randomized phase III study of pegylated liposomal doxorubicin *versus* topotecan, J. Clin. Oncol. 19 (2001) 3312–3322.
[70] W.J. Gradishar, S. Tjulandin, N. Davidson, H. Shaw, N. Desai, P. Bhar, M. Hawkins, J. O'Shaughnessy, Phase III trial of nanoparticle albumin-bound paclitaxel compared with polyethylated castor oil-based paclitaxel in women with breast cancer, J. Clin. Oncol. 23 (2005) 7794–7803.
[71] C. Li, S. Wallace, Polymer-drug conjugates: recent development in clinical oncology, Adv. Drug Deliv. Rev. 60 (2008) 886–898.
[72] R. Jain, J. Gutierrez, J. Narang, L. Scarpace, L.R. Schultz, N. Lemke, S.C. Patel, T. Mikkelsen, J.P. Rock, *In vivo* correlation of tumor blood volume and permeability with histologic and molecular angiogenic markers in gliomas, AJNR Am. J. Neuroradiol. 32 (2011) 388–394.
[73] M.J. Ernsting, W.D. Foltz, E. Undzys, T. Tagami, S.D. Li, Tumor-targeted drug delivery using MR-contrasted docetaxel–carboxymethylcellulose nanoparticles, Biomaterials 33 (2012) 3931–3941.
[74] T. Lammers, F. Kiessling, W.E. Hennink, G. Storm, Drug targeting to tumors: principles, pitfalls and (pre-) clinical progress, J. Control. Release 161 (2) (2012) 175–187.
[75] U. Prabhakar, H. Maeda, R.K. Jain, E.M. Sevick-Muraca, W. Zamboni, O.C. Farokhzad, S.T. Barry, A. Gabizon, P. Grodzinski, D.C. Blakey, Challenges and key considerations of the enhanced permeability and retention effect for nanomedicine drug delivery in oncology, Cancer Res. 73 (2013) 2412–2417.
[76] T. Lammers, F. Kiessling, W.E. Hennink, G. Storm, Drug targeting to tumors: principles, pitfalls and (pre-) clinical progress, J. Control. Release 161 (2012) 175–187.
[77] H. Cabral, Y. Matsumoto, K. Mizuno, Q. Chen, M. Murakami, M. Kimura, Y. Terada, M.R. Kano, K. Miyazono, M. Uesaka, N. Nishiyama, K. Kataoka, Accumulation of sub-100 nm polymeric micelles in poorly permeable tumours depends on size, Nat. Nanotechnol. 6 (2011) 815–823.
[78] H. Lee, H. Fonge, B. Hoang, R.M. Reilly, C. Allen, The effects of particle size and molecular targeting on the intratumoral and subcellular distribution of polymeric nanoparticles, Mol. Pharm. 7 (2010) 1195–1208.
[79] R.K. Jain, Determinants of tumor blood flow: a review, Cancer Res. 48 (1988) 2641–2658.
[80] R.K. Jain, Normalizing tumor vasculature with anti-angiogenic therapy: a new paradigm for combination therapy, Nat. Med. 7 (2001) 987–989.
[81] R.K. Jain, R.T. Tong, L.L. Munn, Effect of vascular normalization by antiangiogenic therapy on interstitial hypertension, peritumor edema, and lymphatic metastasis: insights from a mathematical model, Cancer Res. 67 (2007) 2729–2735.
[82] P. Carmeliet, R.K. Jain, Angiogenesis in cancer and other diseases, Nature 407 (2000) 249–257.
[83] F. Winkler, S.V. Kozin, R.T. Tong, S.S. Chae, M.F. Booth, I. Garkavtsev, L. Xu, D.J. Hicklin, D. Fukumura, E. di Tomaso, L.L. Munn, R.K. Jain, Kinetics of vascular normalization by VEGFR2 blockade governs brain tumor response to radiation: role of oxygenation, angiopoietin-1, and matrix metalloproteinases, Cancer Cell 6 (2004) 553–563.
[84] R.T. Tong, Y. Boucher, S.V. Kozin, F. Winkler, D.J. Hicklin, R.K. Jain, Vascular normalization by vascular endothelial growth factor receptor 2 blockade induces a pressure gradient across the vasculature and improves drug penetration in tumors, Cancer Res. 64 (2004) 3731–3736.
[85] S. Tanaka, T. Akaike, J. Wu, J. Fang, T. Sawa, M. Ogawa, T. Beppu, H. Maeda, Modulation of tumor-selective vascular blood flow and extravasation by the stable prostaglandin 12 analogue beraprost sodium, J. Drug Target. 11 (2003) 45–52.
[86] C.H. Heldin, K. Rubin, K. Pietras, A. Ostman, High interstitial fluid pressure — an obstacle in cancer therapy, Nat. Rev. Cancer 4 (2004) 806–813.
[87] A.L. Seynhaeve, S. Hoving, D. Schipper, C.E. Vermeulen, G. de Wiel-Ambagtsheer, S.T. van Tiel, A.M. Eggermont, T.L. Ten Hagen, Tumor necrosis factor alpha mediates homogeneous distribution of liposomes in murine melanoma that contributes to a better tumor response, Cancer Res. 67 (2007) 9455–9462.
[88] T. Seki, F. Carroll, S. Illingworth, R. Cawood, V. Subr, K.D. Fisher, L.W. Seymour, Tumor necrosis factor-alpha increases extravasation of virus particles into tumor tissue by activating the Rho A/Rho kinase pathway, J. Control. Release 156 (3) (2011) 381–389.
[89] M.R. Kano, Y. Bae, C. Iwata, Y. Morishita, M. Yashiro, M. Oka, T. Fujii, A. Komuro, K. Kiyono, M. Kaminishi, K. Hirakawa, Y. Ouchi, N. Nishiyama, K. Kataoka, K. Miyazono, Improvement of cancer-targeting therapy, using nanocarriers for intractable solid tumors by inhibition of TGF-beta signaling, Proc. Natl. Acad. Sci. U. S. A. 104 (2007) 3460–3465.
[90] L. Davies Cde, L.M. Lundstrom, J. Frengen, L. Eikenes, S.O. Bruland, O. Kaalhus, M.H. Hjelstuen, C. Brekken, Radiation improves the distribution and uptake of liposomal doxorubicin (caelyx) in human osteosarcoma xenografts, Cancer Res. 64 (2004) 547–553.
[91] C. Li, S. Ke, Q.P. Wu, W. Tansey, N. Hunter, L.M. Buchmiller, L. Milas, C. Charnsangavej, S. Wallace, Tumor irradiation enhances the tumor-specific

distribution of poly(L-glutamic acid)-conjugated paclitaxel and its antitumor efficacy, Clin. Cancer Res. 6 (2000) 2829–2834.
[92] M.S. Anscher, L. Chen, Z. Rabbani, S. Kang, N. Larrier, H. Huang, T.V. Samulski, M.W. Dewhirst, D.M. Brizel, R.J. Folz, Z. Vujaskovic, Recent progress in defining mechanisms and potential targets for prevention of normal tissue injury after radiation therapy, Int. J. Radiat. Oncol. Biol. Phys. 62 (2005) 255–259.
[93] J.H. Park, G. von Maltzahn, L. Zhang, M.P. Schwartz, E. Ruoslahti, S.N. Bhatia, M.J. Sailor, Magnetic iron oxide nanoworms for tumor targeting and imaging, Adv. Mater. 20 (2008) 1630–1635.
[94] V.P. Torchilin, A.N. Lukyanov, Z. Gao, B. Papahadjopoulos-Sternberg, Immunomicelles: targeted pharmaceutical carriers for poorly soluble drugs, Proc. Natl. Acad. Sci. U. S. A. 100 (2003) 6039–6044.
[95] M. Choi, K. Choi, S.W. Ryu, J. Lee, C. Choi, Dynamic fluorescence imaging for multiparametric measurement of tumor vasculature, J. Biomed. Opt. 16 (2011) 046008.
[96] H. Lee, B. Hoang, H. Fonge, R.M. Reilly, C. Allen, *In vivo* distribution of polymeric nanoparticles at the whole-body, tumor, and cellular levels, Pharm. Res. 27 (2010) 2343–2355.
[97] S.K. Pal, B.H. Childs, M. Pegram, Triple negative breast cancer: unmet medical needs, Breast Cancer Res. Treat. 125 (2011) 627–636.
[98] R.K. Jain, Transport of molecules in the tumor interstitium: a review, Cancer Res. 47 (1987) 3039–3051.
[99] J.R. Less, M.C. Posner, Y. Boucher, D. Borochovitz, N. Wolmark, R.K. Jain, Interstitial hypertension in human breast and colorectal tumors, Cancer Res. 52 (1992) 6371–6374.
[100] S.D. Nathanson, L. Nelson, Interstitial fluid pressure in breast cancer, benign breast conditions, and breast parenchyma, Ann. Surg. Oncol. 1 (1994) 333–338.
[101] B.D. Curti, W.J. Urba, W.G. Alvord, J.E. Janik, J.W. Smith II, K. Madara, D.L. Longo, Interstitial pressure of subcutaneous nodules in melanoma and lymphoma patients: changes during treatment, Cancer Res. 53 (1993) 2204–2207.
[102] B. Rippe, B. Haraldsson, Transport of macromolecules across microvascular walls: the two-pore theory, Physiol. Rev. 74 (1994) 163–219.
[103] M.J. Ernsting, W.D. Foltz, E. Undzys, T. Tagami, S.D. Li, Tumor-targeted drug delivery using MR-contrasted docetaxel–carboxymethylcellulose nanoparticles, Biomaterials 33 (15) (2012) 3931–3941.
[104] H.F. Dvorak, Tumors: wounds that do not heal. Similarities between tumor stroma generation and wound healing, N. Engl. J. Med. 315 (1986) 1650–1659.
[105] L. Ronnov-Jessen, O.W. Petersen, M.J. Bissell, Cellular changes involved in conversion of normal to malignant breast: importance of the stromal reaction, Physiol. Rev. 76 (1996) 69–125.
[106] R. Kalluri, M. Zeisberg, Fibroblasts in cancer, Nat. Rev. Cancer 6 (2006) 392–401.
[107] A. Aboussekhra, Role of cancer-associated fibroblasts in breast cancer development and prognosis, Int. J. Dev. Biol. 55 (2011) 841–849.
[108] P.A. Netti, D.A. Berk, M.A. Swartz, A.J. Grodzinsky, R.K. Jain, Role of extracellular matrix assembly in interstitial transport in solid tumors, Cancer Res. 60 (2000) 2497–2503.
[109] E.B. Brown, Y. Boucher, S. Nasser, R.K. Jain, Measurement of macromolecular diffusion coefficients in human tumors, Microvasc. Res. 67 (2004) 231–236.
[110] D. Toomey, J. Harmey, C. Condron, E. Kay, D. Bouchier-Hayes, Phenotyping of immune cell infiltrates in breast and colorectal tumours, Immunol. Invest. 28 (1999) 29–41.
[111] H.H. van Ravenswaay Claasen, P.M. Kluin, G.J. Fleuren, Tumor infiltrating cells in human cancer. On the possible role of CD16+ macrophages in antitumor cytotoxicity, Lab. Invest. 67 (1992) 166–174.
[112] B. al-Sarireh, O. Eremin, Tumour-associated macrophages (TAMS): disordered function, immune suppression and progressive tumour growth, J. R. Coll. Surg. Edinb. 45 (2000) 1–16.
[113] S.A. Shaffer, C. Baker-Lee, J. Kennedy, M.S. Lai, P. de Vries, K. Buhler, J.W. Singer, *In vitro* and *in vivo* metabolism of paclitaxel poliglumex: identification of metabolites and active proteases, Cancer Chemother. Pharmacol. 59 (2007) 537–548.
[114] E.F. Jackson, E. Esparza-Coss, X. Wen, C.S. Ng, S.L. Daniel, R.E. Price, B. Rivera, C. Charnsangavej, J.G. Gelovani, C. Li, Magnetic resonance imaging of therapy-induced necrosis using gadolinium-chelated polyglutamic acids, Int. J. Radiat. Oncol. Biol. Phys. 68 (2007) 830–838.
[115] D. Alizadeh, L. Zhang, J. Hwang, T. Schluep, B. Badie, Tumor-associated macrophages are predominant carriers of cyclodextrin-based nanoparticles into gliomas, Nanomedicine 6 (2010) 382–390.
[116] S. Ramanujan, A. Pluen, T.D. McKee, E.B. Brown, Y. Boucher, R.K. Jain, Diffusion and convection in collagen gels: implications for transport in the tumor interstitium, Biophys. J. 83 (2002) 1650–1660.
[117] N.M. La-Beck, B.A. Zamboni, A. Gabizon, H. Schmeeda, M. Amantea, P.A. Gehrig, W.C. Zamboni, Factors affecting the pharmacokinetics of pegylated liposomal doxorubicin in patients, Cancer Chemother. Pharmacol. 69 (2012) 43–50.
[118] T. Stylianopoulos, M.Z. Poh, N. Insin, M.G. Bawendi, D. Fukumura, L.L. Munn, R.K. Jain, Diffusion of particles in the extracellular matrix: the effect of repulsive electrostatic interactions, Biophys. J. 99 (2010) 1342–1349.
[119] O. Lieleg, R.M. Baumgartel, A.R. Bausch, Selective filtering of particles by the extracellular matrix: an electrostatic bandpass, Biophys. J. 97 (2009) 1569–1577.
[120] T. Nomura, N. Koreeda, F. Yamashita, Y. Takakura, M. Hashida, Effect of particle size and charge on the disposition of lipid carriers after intratumoral injection into tissue-isolated tumors, Pharm. Res. 15 (1998) 128–132.
[121] C.G. Willett, Y. Boucher, E. di Tomaso, D.G. Duda, L.L. Munn, R.T. Tong, D.C. Chung, D.V. Sahani, S.P. Kalva, S.V. Kozin, M. Mino, K.S. Cohen, D.T. Scadden, A.C. Hartford, A.J. Fischman, J.W. Clark, D.P. Ryan, A.X. Zhu, L.S. Blaszkowsky, H.X. Chen, P.C. Shellito, G.Y. Lauwers, R.K. Jain, Direct evidence that the VEGF-specific antibody bevacizumab has antivascular effects in human rectal cancer, Nat. Med. 10 (2004) 145–147.
[122] H.I. Hurwitz, L. Fehrenbacher, J.D. Hainsworth, W. Heim, J. Berlin, E. Holmgren, J. Hambleton, W.F. Novotny, F. Kabbinavar, Bevacizumab in combination with fluorouracil and leucovorin: an active regimen for first-line metastatic colorectal cancer, J. Clin. Oncol. 23 (2005) 3502–3508.
[123] H. Wildiers, G. Guetens, G. De Boeck, E. Verbeken, B. Landuyt, W. Landuyt, E.A. de Bruijn, A.T. van Oosterom, Effect of antivascular endothelial growth factor treatment on the intratumoral uptake of CPT-11, Br. J. Cancer 88 (2003) 1979–1986.
[124] K. Pietras, Increasing tumor uptake of anticancer drugs with imatinib, Semin. Oncol. 31 (2004) 18–23.
[125] K. Pietras, A. Ostman, M. Sjoquist, E. Buchdunger, R.K. Reed, C.H. Heldin, K. Rubin, Inhibition of platelet-derived growth factor receptors reduces interstitial hypertension and increases transcapillary transport in tumors, Cancer Res. 61 (2001) 2929–2934.
[126] R. Cairns, I. Papandreou, N. Denko, Overcoming physiologic barriers to cancer treatment by molecularly targeting the tumor microenvironment, Mol. Cancer Res. 4 (2006) 61–70.
[127] M. Murakami, M.J. Ernsting, E. Undzys, N. Holwell, W.D. Foltz, S.D. Li, Docetaxel conjugate nanoparticles that target a-smooth muscle actin–expressing stromal cells suppress breast cancer metastasis, Cancer Res. 73 (15) (2013) 4862–4871.
[128] T.P. Padera, B.R. Stoll, J.B. Tooredman, D. Capen, E. di Tomaso, R.K. Jain, Pathology: cancer cells compress intratumour vessels, Nature 427 (2004) 695.
[129] D.D. Von Hoff, R.K. Ramanathan, M.J. Borad, D.A. Laheru, L.S. Smith, T.E. Wood, R.L. Korn, N. Desai, V. Trieu, J.L. Iglesias, H. Zhang, P. Soon-Shiong, T. Shi, N.V. Rajeshkumar, A. Maitra, M. Hidalgo, Gemcitabine plus nab-paclitaxel is an active regimen in patients with advanced pancreatic cancer: a phase I/II trial, J. Clin. Oncol. 29 (2011) 4548–4554.
[130] K.P. Olive, M.A. Jacobetz, C.J. Davidson, A. Gopinathan, D. McIntyre, D. Honess, B. Madhu, M.A. Goldgraben, M.E. Caldwell, D. Allard, K.K. Frese, G. Denicola, C. Feig, C. Combs, S.P. Winter, H. Ireland-Zecchini, S. Reichelt, W.J. Howat, A. Chang, M. Dhara, L. Wang, F. Ruckert, R. Grutzmann, C. Pilarsky, K. Izeradjene, S.R. Hingorani, P. Huang, S.E. Davies, W. Plunkett, M. Egorin, R.H. Hruban, N. Whitebread, K. McGovern, J. Adams, C. Iacobuzio-Donahue, J. Griffiths, D.A. Tuveson, Inhibition of Hedgehog signaling enhances delivery of chemotherapy in a mouse model of pancreatic cancer, Science 324 (2009) 1457–1461.
[131] D. Hanahan, R.A. Weinberg, Hallmarks of cancer: the next generation, Cell 144 (2011) 646–674.
[132] T.L. Andresen, S.S. Jensen, K. Jorgensen, Advanced strategies in liposomal cancer therapy: problems and prospects of active and tumor specific drug release, Prog. Lipid Res. 44 (2005) 68–97.
[133] K.M. Laginha, S. Verwoert, G.J. Charrois, T.M. Allen, Determination of doxorubicin levels in whole tumor and tumor nuclei in murine breast cancer tumors, Clin. Cancer Res. 11 (2005) 6944–6949.
[134] A. Gabizon, H. Shmeeda, Y. Barenholz, Pharmacokinetics of pegylated liposomal Doxorubicin: review of animal and human studies, Clin. Pharmacokinet. 42 (2003) 419–436.
[135] K.J. Harrington, C.R. Lewanski, A.D. Northcote, J. Whittaker, H. Wellbank, R.G. Vile, A.M. Peters, J.S. Stewart, Phase I–II study of pegylated liposomal cisplatin (SPI-077) in patients with inoperable head and neck cancer, Ann. Oncol. 12 (2001) 493–496.
[136] W.T. Lim, E.H. Tan, C.K. Toh, S.W. Hee, S.S. Leong, P.C. Ang, N.S. Wong, B. Chowbay, Phase I pharmacokinetic study of a weekly liposomal paclitaxel formulation (Genexol-PM) in patients with solid tumors, Ann. Oncol. 21 (2010) 382–388.
[137] T. Hamaguchi, Y. Matsumura, M. Suzuki, K. Shimizu, R. Goda, I. Nakamura, I. Nakatomi, M. Yokoyama, K. Kataoka, T. Kakizoe, NK105, a paclitaxel-incorporating micellar nanoparticle formulation, can extend *in vivo* antitumour activity and reduce the neurotoxicity of paclitaxel, Br. J. Cancer 92 (2005) 1240–1246.
[138] G. Gaucher, R.H. Marchessault, J.C. Leroux, Polyester-based micelles and nanoparticles for the parenteral delivery of taxanes, J. Control. Release 143 (2010) 2–12.
[139] K. Letchford, R. Liggins, K.M. Wasan, H. Burt, *In vitro* human plasma distribution of nanoparticulate paclitaxel is dependent on the physicochemical properties of poly(ethylene glycol)-block-poly(caprolactone) nanoparticles, Eur. J. Pharm. Biopharm. 71 (2009) 196–206.
[140] E. Miele, G.P. Spinelli, F. Tomao, S. Tomao, Albumin-bound formulation of paclitaxel (Abraxane ABI-007) in the treatment of breast cancer, Int. J. Nanomedicine 4 (2009) 99–105.
[141] M. Harries, P. Ellis, P. Harper, Nanoparticle albumin-bound paclitaxel for metastatic breast cancer, J. Clin. Oncol. 23 (2005) 7768–7771.
[142] D.W. Nyman, K.J. Campbell, E. Hersh, K. Long, K. Richardson, V. Trieu, N. Desai, M.J. Hawkins, D.D. Von Hoff, Phase I and pharmacokinetics trial of ABI-007, a novel nanoparticle formulation of paclitaxel in patients with advanced nonhematologic malignancies, J. Clin. Oncol. 23 (2005) 7785–7793.
[143] A.V. Boddy, E.R. Plummer, R. Todd, J. Sludden, M. Griffin, L. Robson, J. Cassidy, D. Bissett, A. Bernareggi, M.W. Verrill, A.H. Calvert, A phase I and pharmacokinetic study of paclitaxel poliglumex (XYOTAX), investigating both 3-weekly and 2-weekly schedules, Clin. Cancer Res. 11 (2005) 7834–7840.
[144] C. Li, R.A. Newman, Q.P. Wu, S. Ke, W. Chen, T. Hutto, Z. Kan, M.D. Brannan, C. Charnsangavej, S. Wallace, Biodistribution of paclitaxel and poly(L-glutamic acid)-paclitaxel conjugate in mice with ovarian OCa-1 tumor, Cancer Chemother. Pharmacol. 46 (2000) 416–422.
[145] S.D. Conner, S.L. Schmid, Regulated portals of entry into the cell, Nature 422 (2003) 37–44.
[146] F. Zhao, Y. Zhao, Y. Liu, X. Chang, C. Chen, Y. Zhao, Cellular uptake, intracellular trafficking, and cytotoxicity of nanomaterials, Small 7 (2011) 1322–1337.
[147] J. Wang, J.D. Byrne, M.E. Napier, J.M. DeSimone, More effective nanomedicines through particle design, Small 7 (2011) 1919–1931.
[148] T.M. Allen, P.R. Cullis, Liposomal drug delivery systems: from concept to clinical applications, Adv. Drug Deliv. Rev. 65 (2013) 36–48.

[149] A. Koshkaryev, R. Sawant, M. Deshpande, V. Torchilin, Immunoconjugates and long circulating systems: origins, current state of the art and future directions, Adv. Drug Deliv. Rev. 65 (2013) 24–35.
[150] A.S. Hoffman, Stimuli-responsive polymers: biomedical applications and challenges for clinical translation, Adv. Drug Deliv. Rev. 65 (2013) 10–16.
[151] W. Arap, W. Haedicke, M. Bernasconi, R. Kain, D. Rajotte, S. Krajewski, H.M. Ellerby, D.E. Bredesen, R. Pasqualini, E. Ruoslahti, Targeting the prostate for destruction through a vascular address, Proc. Natl. Acad. Sci. U. S. A. 99 (2002) 1527–1531.
[152] S.E. Gratton, P.A. Ropp, P.D. Pohlhaus, J.C. Luft, V.J. Madden, M.E. Napier, J.M. DeSimone, The effect of particle design on cellular internalization pathways, Proc. Natl. Acad. Sci. U. S. A. 105 (2008) 11613–11618.
[153] W. Jiang, B.Y. Kim, J.T. Rutka, W.C. Chan, Nanoparticle-mediated cellular response is size-dependent, Nat. Nanotechnol. 3 (2008) 145–150.
[154] X. Huang, X. Teng, D. Chen, F. Tang, J. He, The effect of the shape of mesoporous silica nanoparticles on cellular uptake and cell function, Biomaterials 31 (2010) 438–448.
[155] B.D. Chithrani, A.A. Ghazani, W.C. Chan, Determining the size and shape dependence of gold nanoparticle uptake into mammalian cells, Nano Lett. 6 (2006) 662–668.
[156] K. Zhang, H. Fang, Z. Chen, J.S. Taylor, K.L. Wooley, Shape effects of nanoparticles conjugated with cell-penetrating peptides (HIV Tat PTD) on CHO cell uptake, Bioconjug. Chem. 19 (2008) 1880–1887.
[157] X. Guo, F.C. Szoka Jr., Steric stabilization of fusogenic liposomes by a low-pH sensitive PEG–diortho ester–lipid conjugate, Bioconjug. Chem. 12 (2001) 291–300.
[158] A.A. Kale, V.P. Torchilin, Enhanced transfection of tumor cells *in vivo* using "Smart" pH-sensitive TAT-modified pegylated liposomes, J. Drug Target. 15 (2007) 538–545.
[159] L. Zhu, P. Kate, V.P. Torchilin, Matrix metalloprotease 2-responsive multifunctional liposomal nanocarrier for enhanced tumor targeting, ACS Nano 6 (2012) 3491–3498.
[160] S.C. Semple, A. Akinc, J. Chen, A.P. Sandhu, B.L. Mui, C.K. Cho, D.W. Sah, D. Stebbing, E.J. Crosley, E. Yaworski, I.M. Hafez, J.R. Dorkin, J. Qin, K. Lam, K.G. Rajeev, K.F. Wong, L.B. Jeffs, L. Nechev, M.L. Eisenhardt, M. Jayaraman, M. Kazem, M.A. Maier, M. Srinivasulu, M.J. Weinstein, Q. Chen, R. Alvarez, S.A. Barros, S. De, S.K. Klimuk, T. Borland, V. Kosovrasti, W.L. Cantley, Y.K. Tam, M. Manoharan, M.A. Ciufolini, M.A. Tracy, A. de Fougerolles, I. MacLachlan, P.R. Cullis, T.D. Madden, M.J. Hope, Rational design of cationic lipids for siRNA delivery, Nat. Biotechnol. 28 (2010) 172–176.
[161] T. Osaka, T. Nakanishi, S. Shanmugam, S. Takahama, H. Zhang, Effect of surface charge of magnetite nanoparticles on their internalization into breast cancer and umbilical vein endothelial cells, Colloids Surf. B Biointerfaces 71 (2009) 325–330.
[162] A. Santel, M. Aleku, O. Keil, J. Endruschat, V. Esche, G. Fisch, S. Dames, K. Loffler, M. Fechtner, W. Arnold, K. Giese, A. Klippel, J. Kaufmann, A novel siRNA-lipoplex technology for RNA interference in the mouse vascular endothelium, Gene Ther. 13 (2006) 1222–1234.
[163] T.H. Chung, S.H. Wu, M. Yao, C.W. Lu, Y.S. Lin, Y. Hung, C.Y. Mou, Y.C. Chen, D.M. Huang, The effect of surface charge on the uptake and biological function of mesoporous silica nanoparticles in 3T3-L1 cells and human mesenchymal stem cells, Biomaterials 28 (2007) 2959–2966.
[164] S.D. Li, L. Huang, Nanoparticles evading the reticuloendothelial system: role of the supported bilayer, Biochim. Biophys. Acta 1788 (2009) 2259–2266.
[165] I. Maclachlan, P. Cullis, Diffusible-PEG-lipid stabilized plasmid lipid particles, Adv. Genet. 53PA (2005) 157–188.
[166] J.S. Choi, J.A. MacKay, F.C. Szoka Jr., Low-pH-sensitive PEG-stabilized plasmid-lipid nanoparticles: preparation and characterization, Bioconjug. Chem. 14 (2003) 420–429.
[167] D.B. Kirpotin, D.C. Drummond, Y. Shao, M.R. Shalaby, K. Hong, U.B. Nielsen, J.D. Marks, C.C. Benz, J.W. Park, Antibody targeting of long-circulating lipidic nanoparticles does not increase tumor localization but does increase internalization in animal models, Cancer Res. 66 (2006) 6732–6740.
[168] K. McNeeley, A. Annapragada, R. Bellamkonda, Decreased circulation time offsets increased efficacy of PEGylated nanocarriers targeting folate receptors of glioma, Nanotechnology 18 (2007) 385101.
[169] W.C. Chen, G.C. Completo, D.S. Sigal, P.R. Crocker, A. Saven, J.C. Paulson, *In vivo* targeting of B-cell lymphoma with glycan ligands of CD22, Blood 115 (2010) 4778–4786.
[170] S. Muro, New biotechnological and nanomedicine strategies for treatment of lysosomal storage disorders, Wiley Interdiscip. Rev. Nanomed. Nanobiotechnol. 2 (2010) 189–204.
[171] D.W. Bartlett, H. Su, I.J. Hildebrandt, W.A. Weber, M.E. Davis, Impact of tumor-specific targeting on the biodistribution and efficacy of siRNA nanoparticles measured by multimodality *in vivo* imaging, Proc. Natl. Acad. Sci. U. S. A. 104 (2007) 15549–15554.
[172] S.H. Pun, F. Tack, N.C. Bellocq, J. Cheng, B.H. Grubbs, G.S. Jensen, M.E. Davis, M. Brewster, M. Janicot, B. Janssens, W. Floren, A. Bakker, Targeted delivery of RNA-cleaving DNA enzyme (DNAzyme) to tumor tissue by transferrin-modified, cyclodextrin-based particles, Cancer Biol. Ther. 3 (2004) 641–650.
[173] S.D. Li, Y.C. Chen, M.J. Hackett, L. Huang, Tumor-targeted delivery of siRNA by self-assembled nanoparticles, Mol. Ther. 16 (2008) 163–169.
[174] W.C. Zamboni, J.L. Eiseman, S. Strychor, P.M. Rice, E. Joseph, B.A. Zamboni, M.K. Donnelly, J. Shurer, R.A. Parise, M.E. Tonda, N.Y. Yu, P.H. Basse, Tumor disposition of pegylated liposomal CKD-602 and the reticuloendothelial system in preclinical tumor models, J. Liposome Res. 21 (2011) 70–80.
[175] S.D. Li, L. Huang, Stealth nanoparticles: high density but sheddable PEG is a key for tumor targeting, J. Control. Release 145 (2010) 178–181.
[176] Y. Yang, J. Li, F. Liu, L. Huang, Systemic delivery of siRNA *via* LCP nanoparticle efficiently inhibits lung metastasis, Mol. Ther. 20 (2012) 609–615.
[177] W.P. Caron, G. Song, P. Kumar, S. Rawal, W.C. Zamboni, Interpatient pharmacokinetic and pharmacodynamic variability of carrier-mediated anticancer agents, Clin. Pharmacol. Ther. 91 (2012) 802–812.
[178] E. Karathanasis, S. Suryanarayanan, S.R. Balusu, K. McNeeley, I. Sechopoulos, A. Karellas, A.V. Annapragada, R.V. Bellamkonda, Imaging nanoprobe for prediction of outcome of nanoparticle chemotherapy by using mammography, Radiology 250 (2009) 398–406.
[179] T. Tagami, M.J. Ernsting, S.D. Li, Efficient tumor regression by a single and low dose treatment with a novel and enhanced formulation of thermosensitive liposomal doxorubicin, J. Control. Release 152 (2011) 303–309.
[180] T. Tagami, M.J. Ernsting, S.D. Li, Optimization of a novel and improved thermosensitive liposome formulated with DPPC and a Brij surfactant using a robust *in vitro* system, J. Control. Release 154 (2011) 290–297.
[181] T. Tagami, W.D. Foltz, M.J. Ernsting, C.M. Lee, I.F. Tannock, J.P. May, S.D. Li, MRI monitoring of intratumoral drug delivery and prediction of the therapeutic effect with a multifunctional thermosensitive liposome, Biomaterials 32 (2011) 6570–6578.
[182] T. Tagami, J.P. May, M.J. Ernsting, S.D. Li, A thermosensitive liposome prepared with a Cu2+ gradient demonstrates improved pharmacokinetics, drug delivery and antitumor efficacy, J. Control. Release 161 (1) (2012) 142–149.
[183] D. Needham, M.W. Dewhirst, The development and testing of a new temperature-sensitive drug delivery system for the treatment of solid tumors, Adv. Drug Deliv. Rev. 53 (2001) 285–305.
[184] A.B. Simonson, J.E. Schnitzer, Vascular proteomic mapping *in vivo*, J. Thromb. Haemost. 5 (Suppl. 1) (2007) 183–187.